Evaluation of Corrosion Resistance of Different Steel Reinforcement Types

Final Report
May 2006

Sponsored by
the Iowa Department of Transportation
(CTRE Project 02-103)

IOWA STATE UNIVERSITY

About the Bridge Engineering Center

The mission of the Bridge Engineering Center is to conduct research on bridge technologies to help bridge designers/owners design, build, and maintain long-lasting bridges.

Disclaimer Notice

The contents of this report reflect the views of the authors, who are responsible for the facts and the accuracy of the information presented herein. The opinions, findings and conclusions expressed in this publication are those of the authors and not necessarily those of the sponsors.

The sponsors assume no liability for the contents or use of the information contained in this document. This report does not constitute a standard, specification, or regulation.

The sponsors do not endorse products or manufacturers. Trademarks or manufacturers' names appear in this report only because they are considered essential to the objective of the document.

Nondiscrimination Statement

Iowa State University does not discriminate on the basis of race, color, age, religion, national origin, sexual orientation, gender identity, sex, marital status, disability, or status as a U.S. veteran. Inquiries can be directed to the Director of Equal Opportunity and Diversity, (515) 294-7612.

Technical Report Documentation Page

1. Report No. CTRE Project 02-103	**2. Government Accession No.**	**3. Recipient's Catalog No.**	
4. Title and Subtitle Evaluation of Corrosion Resistance of Different Steel Reinforcement Types		**5. Report Date** May 2006	
		6. Performing Organization Code	
7. Author(s) Brent M. Phares, Fouad S. Fanous, Terry J. Wipf, Yoon-Si Lee, Milan J. Jolley		**8. Performing Organization Report No.**	
9. Performing Organization Name and Address Center for Transportation Research and Education Iowa State University 2711 South Loop Drive, Suite 4700 Ames, IA 50010-8664		**10. Work Unit No. (TRAIS)**	
		11. Contract or Grant No.	
12. Sponsoring Organization Name and Address Iowa Department of Transportation 800 Lincoln Way Ames, IA 50010		**13. Type of Report and Period Covered** Final Report	
		14. Sponsoring Agency Code	
15. Supplementary Notes Visit www.ctre.iastate.edu for color PDF files of this and other research reports.			

16. Abstract

The corrosion of steel reinforcement in an aging highway infrastructure is a major problem currently facing the transportation engineering community. In the United States alone, maintenance and replacement costs for deficient bridges are measured in billions of dollars. The application of corrosion-resistant steel reinforcement as an alternative reinforcement to existing mild steel reinforced concrete bridge decks has potential to mitigate corrosion problems, due to the fundamental properties associated with the materials.

To investigate corrosion prevention through the use of corrosion-resistant alloys, the performance of corrosion resistance of MMFX microcomposite steel reinforcement, a high-strength, high-chromium steel reinforcement, was evaluated. The study consisted of both field and laboratory components conducted at the Iowa State University Bridge Engineering Center to determine whether MMFX reinforcement provides superior corrosion resistance to epoxy-coated mild steel reinforcement in bridge decks. Because definitive field evidence of the corrosion resistance of MMFX reinforcement may require several years of monitoring, strict attention was given to investigating reinforcement under accelerated conditions in the laboratory, based on typical ASTM and Rapid Macrocell accelerated corrosion tests.

After 40 weeks of laboratory testing, the ASTM ACT corrosion potentials indicate that corrosion had not initiated for either MMFX or the as-delivered epoxy-coated reinforcement. Conversely, uncoated mild steel specimens underwent corrosion within the fifth week, while epoxy-coated reinforcement specimens with induced holidays underwent corrosion between 15 and 30 weeks. Within the fifth week of testing, the Rapid Macrocell ACT produced corrosion risk potentials that indicate active corrosion for all reinforcement types tested. While the limited results from the 40 weeks of laboratory testing may not constitute a prediction of life expectancy and life-cycle cost, a procedure is presented herein to determine life expectancy and associated life-cycle costs.

17. Key Words accelerated corrosion testing— bridge deck reinforcement corrosion—epoxy-coated steel reinforcement—MMFX microcomposite steel reinforcement		**18. Distribution Statement** No restrictions.	
19. Security Classification (of this report) Unclassified.	**20. Security Classification (of this page)** Unclassified.	**21. No. of Pages** 79	**22. Price** NA

Form DOT F 1700.7 (8-72) **Reproduction of completed page authorized**

EVALUATION OF CORROSION RESISTANCE OF DIFFERENT STEEL REINFORCEMENT TYPES

Final Report
May 2006

Co-Principal Investigators
Terry J. Wipf
Professor of Civil Engineering, Iowa State University
Director of the Bridge Engineering Center, Center for Transportation Research and Education

Brent M. Phares
Associate Director, Bridge Engineering Center, Center for Transportation Research and Education

Fouad S. Fanous
Professor of Civil Engineering, Iowa State University

Research Assistants
Yoon-Si Lee, Milan J. Jolley

Preparation of this report was financed in part
through funds provided by the Iowa Department of Transportation
through its research management agreement with the
Center for Transportation Research and Education,
CTRE Project 02-103.

A report from
Center for Transportation Research and Education
Iowa State University
2711 South Loop Drive, Suite 4700
Ames, IA 50010-8664
Phone: 515-294-8103
Fax: 515-294-0467
www.ctre.iastate.edu

TABLE OF CONTENTS

LIST OF FIGURES

LIST OF TABLES

ACKNOWLEDGMENTS

The investigation presented in this report was conducted by the Center for Transportation Research and Education, Bridge Engineering Center. The research was sponsored by the Iowa Department of Transportation (Iowa DOT) through the Federal Highway Administration (FHWA), Innovative Bridge Research and Construction Program.

The authors would like to thank the Iowa Division of the FHWA for their support on this project and extend sincere appreciation to the numerous Iowa DOT personnel, especially those in the Offices of Bridges and Structures and Maintenance who provided significant assistance. Special thanks are extended to Curtis Monk (FHWA, Iowa division bridge engineer), Ahmad Abu-Hawash (Iowa DOT chief structural engineer), and Norman McDonald (Iowa DOT bridge engineer) for their help in various phases of the project. Special thanks are also accorded to Douglas L. Wood (Iowa State University Structural Engineering Laboratory Manager) for his assistance with the installation of the system in the field as well as in the laboratory.

EXECUTIVE SUMMARY

The corrosion of steel reinforcement in an aging highway infrastructure is a major problem now facing the transportation engineering community. In particular, the use of deicing salts has resulted in the steady deterioration of bridge decks due to corrosion. In the United States alone, maintenance and replacement costs for deficient bridges are measured in billions of dollars.

These concerns have initiated the continual development of protective measures for reinforced concrete structures. The application of corrosion-resistant steel reinforcement as an alternative reinforcement to existing mild steel reinforced concrete bridge decks has potential, due to the fundamental properties associated with the materials.

To investigate corrosion prevention through the use of corrosion-resistant alloys, the corrosion resistance of MMFX microcomposite steel reinforcement, a high-strength, high-chromium steel reinforcement, is being evaluated. The study consists of both field and laboratory components conducted at the Iowa State University Bridge Engineering Center to determine whether MMFX reinforcement, in fact, provides superior corrosion resistance to epoxy-coated mild steel reinforcement in bridge decks. Because definitive field evidence of the corrosion resistance of MMFX reinforcement may require several years of monitoring, strict attention was given to investigating reinforcement under accelerated conditions in the laboratory. In the laboratory investigation, the evaluation process was based on typical ASTM and Rapid Macrocell accelerated corrosion tests.

After 40 weeks of laboratory testing, the associated ASTM ACT corrosion potentials indicate that corrosion had not initiated for either MMFX or the as-delivered epoxy-coated reinforcement. Conversely, uncoated mild steel specimens underwent corrosion within the fifth week, while epoxy-coated reinforcement specimens with induced holidays underwent corrosion between 15 and 30 weeks. Within the fifth week of testing, the Rapid Macrocell ACT produced corrosion risk potentials that indicate active corrosion for all reinforcement types tested. For the study presented herein, concrete powder specimens were collected at the top reinforcement depth at the first indication of corrosion. For uncoated mild reinforcement, a chloride ion concentration of 0.63 kg/m^3 (1.06 lb./cu. yd.) was obtained at corrosion initiation. This value correlates with the 0.59 to 0.83 kg/m^3 (1.00 to 1.40 lb./cu. yd.) value commonly believed to be the chloride threshold of uncoated mild steel. For the epoxy-coated reinforcement with induced holidays, the chloride ion concentration at corrosion initiation was measured as 1.03 kg/m^3 (1.74 lb./cu. yd.).

While the limited results from the 40 weeks of laboratory testing may not predict life expectancy and life-cycle cost, a procedure is presented herein to determine life expectancy and associated life-cycle cost. In this life prediction methodology, the life expectancy of bridge decks constructed with different steel reinforcing systems is estimated by a two-stage diffusion-spalling model (i.e., the time required for corrosion initiation plus the subsequent time required to cause spalling due to production of corrosion products). Fick's Second Law of Diffusion was used in this model to estimate the time required for corrosion initiation, while calculated corrosion rates were used to determine the time between corrosion initiation and concrete spalling. The combination of time to initiation and time to spalling results in the time to the first repair.

1. INTRODUCTION

1.1. Background

Reinforced concrete (RC) is a versatile, economical, and proven construction material. Able to be placed in a variety of shapes and finishes, reinforced concrete generally performs well throughout its service life. However, the corrosion of steel reinforcement is the primary and most costly form of deterioration currently impacting the performance of RC bridge structures. For example, in the United States alone this deterioration results in billions of dollars spent to maintain and replace existing bridge decks. In 1979, an estimated $6.3 billion in federal aid was allocated for rehabilitation due to corrosion-induced bridge damage (Locke 1986). By 1986, that amount had risen to $20 billion, and in 1992 the amount totaled $51 billion (Cady and Gannon 1992; Fliz et al. 1992). With ever increasing bridge maintenance costs, protective measures to arrest chloride-induced corrosion have been actively studied for over 30 years.

Eliminating or slowing the deterioration of RC structures due to the corrosion of steel reinforcement requires the use of innovative methodologies, which are commonly subdivided into two categories. First, deterioration is slowed through methods that lengthen the time it takes chloride ions to reach the steel reinforcement. The second includes methods that lengthen the time between initiation of corrosion and the end of service life (Darwin et al. 2002).

Over the last three decades, the principle techniques for corrosion prevention in bridge decks have incorporated increased concrete cover depth and the application of epoxy coating over the steel reinforcement. In 1976, the Iowa Department of Transportation implemented epoxy-coated mild steel reinforcement for the top layer of reinforcement in bridge decks. Within ten years, bridge deck designs had integrated epoxy-coated reinforcement in both the top and bottom layers of reinforcement (Fanous, Wu, and Pape 2000).

Increasing concrete cover depth and infusing epoxy coating over uncoated mild steel reinforcement are believed to delay corrosion initiation and extend service life (Darwin et al. 2002). Increased concrete cover depth lengthens the time for chlorides to propagate to the level of the steel reinforcement and lessens the availability of oxygen and moisture for the corrosion process. However, increasing concrete cover depth increases both dead load and construction costs and is generally unnecessary for structural reasons. Epoxy coatings limit the exposure of the steel to chlorides, oxygen, and moisture. Even in regions with holidays (i.e., areas where the epoxy coating is absent), the corrosion process is thought to be abated because the epoxy coating limits the oxygen and moisture, despite the chloride contact (Darwin et al. 2002). Epoxy-coated reinforcement adds only slightly to the cost of bridge construction. However, some believe that holidays in the epoxy coating at cracked locations, in combination with high chloride concentrations, could result in corrosion of the steel reinforcement that affects the overall performance of the bridge. Furthermore, it is believed that as a bridge deck ages, epoxy coatings may become brittle and eventually, under exposure to high chloride concentrations, delaminate from the steel reinforcement (Smith and Virmani 1996). Small breaks, cracks, etc. in the epoxy coating allow the bond between the coating and steel to be lost. In these cases, the epoxy coating remains generally intact, but the chloride concentration increases in the solution directly below the coating in an environment that is low in oxygen. This results in hydrochloric acid attack of

the steel. An example of this occurred in 1986 when, six years after construction, epoxy-coated reinforcement used in bridge substructures in the Florida Keys showed signs of chloride-induced corrosion (Sagues, Powers, and Locke 1994). This provided an initial indication that the long-term protection provided by epoxy coating may be less than was intended. Furthermore, evidence suggests that, given enough time, even well-applied epoxy coatings tend to lose adhesion by the time chlorides reach the level of the steel reinforcement (Smith and Virmani 1996; Manning 1996).

The above concerns have resulted in the continual development of protective measures. The use of dense concretes, corrosion inhibitors, and both nonmetallic and steel-alloy corrosion-resistant reinforcement are among the most common techniques being considered.

1.2. Objectives

This report presents a dual-phase investigation at Iowa State University that is funded by the Iowa Department of Transportation (Iowa DOT) through the Federal Highway Administration's (FHWA) Innovative Bridge Research and Construction (IBRC) Program. The objective of this study was to determine whether MMFX microcomposite steel reinforcement provides superior corrosion resistance to epoxy-coated mild steel reinforcement (ECR) in bridge decks. The principal reason for selecting a new reinforcement material for concrete bridge decks is to improve both the life expectancy and cost effectiveness of the structural system. A prerequisite is that the material (MMFX steel in this case), which is presumably more expensive than the current material (ECR in this case), provides a significant improvement in corrosion resistance over the current material of choice.

This investigation is comprised of both field and laboratory evaluations of MMFX, epoxy-coated reinforcement, and uncoated reinforcement. Two side-by-side twin bridge decks reinforced with MMFX and epoxy-coated steel were constructed and instrumented to investigate the field performance through periodic monitoring for corrosion initiation and rate. Because the field evaluation may require several years of monitoring to make a valid comparison, tests to accelerate corrosion in a laboratory setting were also conducted. To evaluate corrosion resistance, concrete specimens reinforced with MMFX, epoxy-coated steel, and uncoated steel were constructed and were monitored for corrosion. Traditional mechanical property tests were also conducted to establish the basic mechanical/structural properties.

In both the field and laboratory evaluations, the emphasis of the experimental study was placed on evaluating corrosion resistance performance, including the following:

- Determining the initiation of corrosion and the rate of corrosion growth
- Assessing the difference in corrosion resistance between MMFX, epoxy-coated reinforcement, and uncoated reinforcement

1.3. Tasks

To accomplish the stated objectives, the following tasks were completed:

1. Review related literature: Prior studies related to MMFX reinforcement and corrosion resistance were reviewed to provide background information for evaluating the properties of this new steel type.
2. Conduct field evaluation: The overall field evaluation program consisted of construction documentation and post-construction monitoring of two side-by-side bridges constructed using MMFX and epoxy-coated reinforcement. Sensors were installed in the two newly constructed concrete bridge decks at various critical locations. Periodic measurements were made to assess the corrosion performance of the two bridges.
3. Conduct mechanical laboratory tests: Representative MMFX, epoxy-coated reinforcement, and uncoated reinforcement samples were tested in the laboratory to establish the mechanical properties of each type of steel reinforcement.
4. Conduct laboratory tests for corrosion resistance: In the controlled laboratory environment, ASTM G 109 and Rapid Macrocell accelerated corrosion tests were conducted to evaluate the general and pit corrosion properties of MMFX, epoxy-coated reinforcement, and uncoated reinforcement. At the onset of corrosion, a chloride ion concentration analysis was also performed by testing concrete powder samples.
5. Compile and analyze data: Following testing, Macrocell and half-cell potential change measurements were compiled to determine corrosion rates statistically for each reinforcement type. Comparisons of the corrosion rate and chloride concentration were made between MMFX, epoxy-coated reinforcement, and uncoated reinforcement.
6. Evaluate the performance of MMFX steel as concrete reinforcement: The results of the laboratory corrosion evaluation were combined with analytical and experimental field experience in the state of Iowa to evaluate the impact of the new steel reinforcement on the life expectancy and lifecycle cost of reinforced concrete bridge decks. The life expectancy was modeled as a two-stage process: the time to corrosion initiation and the time from corrosion initiation to spalling). Then, using in-place costs, the lifecycle cost for a bridge deck was calculated.

1.4. Report Layout

This report consists of two parts. Part I gives detailed information regarding the field evaluation program. In this report, instrumentation configuration, data collected, and the overall findings are summarized. The laboratory test program is detailed in Part II. This detail includes an overall summary and the conclusions developed from both the field and laboratory tests. Recommendations for future work are given at the end of this report.

2. LITERATURE REVIEW

2.1. Corrosion Process

Both mild and high-strength steel reinforcement corrode in the presence of oxygen and water. As concrete generally has interconnected pores, air and moisture are ever present around the reinforcement. Initially, at least, the alkaline nature of the surrounding concrete naturally prevents embedded steel reinforcement from corroding. Specifically, microscopic pores within the concrete matrix with high concentrations of soluble calcium, sodium, and potassium oxide form hydroxide when water is present. This process subsequently creates this alkaline condition (i.e., pH 12–13) (Broomfield 1997). The alkaline condition leads to the formation of a "passive" layer on the steel reinforcement surface. This passive layer is a dense, impenetrable film that, if fully established and maintained, prevents further corrosion of the steel reinforcement. A true passive layer is a very dense, thin layer of oxide that leads to a very slow rate of corrosion (Broomfield 1997). The passive layer formed on steel reinforcement in concrete is most likely part metal oxide-hydroxide and part mineral from the cement paste. There is some discussion as to whether this layer is a true passive layer, as it is thick compared to other known passive layers and consists of more than just metal oxides. However, it behaves similarly to a passive layer and, therefore, is generally referred to as such.

Corrosion engineers try to stop the corrosion of steel by simulating the naturally occurring, yet fragile, passive layer with applied protective coatings. Metals such as zinc or polymers such as acrylics and epoxies are sometimes used to stop corrosive conditions from reaching the steel surfaces. The true passive layer is the ideal protective coating, as it will form, maintain, and repair itself as long as the alkaline environment is sustained. This is a far better situation than any artificial coating, as artificial coatings can be consumed or damaged, allowing corrosion to proceed in damaged areas. However, in reality the passive environment is not always maintained in RC. Most notably, the chloride attack mechanism can break down the alkaline condition in concrete, resulting in a corrosion-susceptible environment.

2.1.1. Chloride Attack Mechanism

In structures, chloride ions can come from several sources. They can be cast into the concrete or they can come from the deliberate addition of chlorides. Calcium chloride, for example, was widely used until the mid-1970s as a concrete set accelerator (Broomfield 1997). The use of sea water or sea-dredged aggregate can also contaminate the concrete mix with chloride. Chlorides can also diffuse into concrete as a result of deicing salt application, marine salt spray, and storage of salts.

The diffusion of chlorides via the application of deicing salts or marine salt spray is the primary source of chlorides in most modern RC structures. However, cast-in chloride must not be overlooked. Even a low level of cast-in chloride can lead to the rapid onset of corrosion if additional chlorides become available from the environment. This often happens in marine conditions, where seawater contaminates the original concrete mix and diffuses into the hardened concrete.

Chloride ions penetrate through concrete capillaries and can act as catalysts to corrosion when ion concentration is sufficient at the reinforcement surface. This could break down the passive layer of oxide on the steel, allowing corrosion to initiate. Chloride attack is difficult to remedy, as chlorides are generally hard to eliminate once introduced into a RC structure.

2.1.2. Chloride Threshold

A small concentration of chloride ions in concrete pore water will not break down the previously described passive layer, especially if the system is effectively reestablishing itself. However, there is a chloride threshold for corrosion, given in terms of the chloride-hydroxyl ratio, which represents the concentration of chloride ions required to initiate corrosion. Several researchers have studied uncoated reinforcement in laboratory tests with calcium hydroxide solutions to establish the chloride threshold.

For uncoated mild steel reinforcement, when the chloride concentration exceeds 0.6 of the hydroxyl concentration, corrosion is routinely observed (Hausmann 1967). This approximates to a concentration of 0.4% chloride by weight of cement if chlorides are cast into concrete and 0.2% if they diffuse into concrete (Clear 1975; Clear 1976). Based on an assumed 5 sacks of cement per cubic meter of concrete (6.5 sacks of cement per cubic yard), the chloride threshold for uncoated reinforcement has been estimated to be 0.71 kg/m^3 (1.2 lb./cu. yd.) of concrete (Weyers et al. 1997; Weyers 1995).

Unlike for uncoated reinforcement, no published literature presents definitive chloride threshold values for MMFX microcomposite or epoxy-coated mild steel reinforcement. This may be due to several factors, such as uncertainties associated with the quality of the organic coating of the epoxy, damage that may have occurred during transportation or storage of the epoxy-coated reinforcement, or loss of adhesion between the coating and the base metal. For these reasons, a range of chloride threshold from 1.96 to 2.14 kg/m^3 (3.3 to 3.6 lb./cu. yd.) and 0.71 to 2.14 kg/m^3 (1.2 to 3.6 lb./cu. yd.) at the reinforcement level has been suggested, respectively, for MMFX and epoxy-coated reinforcement (Darwin et al. 2002; Sagues 1994). The lower limit of the range for epoxy-coated reinforcement represents an empirical chloride threshold for uncoated reinforcement (Clear 1975; Clear 1976).

2.1.3. Corrosion Process

Corrosion of steel reinforcement in concrete can generally be modeled as a two-stage process. The first stage is known as the initiation, diffusion, or incubation period, in which chloride ions migrate from the concrete surface to the reinforcement level. During this stage, the reinforcing steel experiences negligible corrosion. The time required for the chloride concentration to reach the aforementioned chloride threshold value at the reinforcement level can be determined by the diffusion process of the chloride ion through concrete, following Fick's Second Law of Diffusion (Weyers, Prowell, and Springkel 1993; Gaal, van der Veen, and Djorai 2001).

Once the passive layer breaks down (i.e., the chloride threshold has been reached), the second stage, which is referred to as the active corrosion period of steel reinforcement, occurs and propagates. The length of the second stage depends on the speed at which the corroded steel reinforcement deteriorates and results in observable distress. Although it is not an easy task to

predict the length of the second stage, eventually a RC structure will reach a condition at which some type of maintenance must be performed.

When corrosion occurs, the steel reinforcement basically "dissolves" in the pore water, giving up electrons and forming cations (positively charged ions). The process of losing electrons is known as oxidation. The following chemical reaction represents the fundamental oxidation of steel reinforcement at the anode (the location that releases electrons).

The anodic reaction: $Fe \rightarrow Fe^{2+} + 2e^{-}$ (2.1)

where *Fe* is iron, Fe^{2+} is ferrous-ion, and $2e^{-}$ are two free electrons.

In the presence of water molecules and the free electrons, oxygen is transformed from a neutral molecule to an anion, which has become more negatively charged by gaining released electrons. This process is called reduction. The gain of electrons comes from a loss of electrons from two substances that react with each other. The following chemical equation illustrates the cathodic reaction (the reaction at the location that gains electrons).

The cathodic reaction: $4e^{-} + 2H_2O + O_2 \rightarrow 4OH^{-}$ (2.2)

where O_2 is oxygen, H_2O is water, and OH^{-} is a hydroxyl ion.

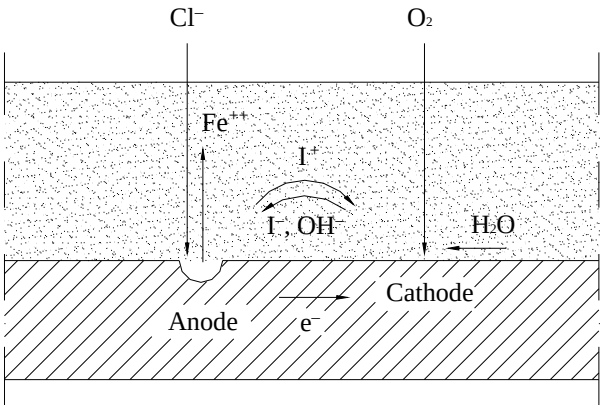

Figure 2.1. Schematic of the corrosion process

The surface of the iron, at which oxidation occurs, serves as an anode. The two free electrons, $2e^{-}$, created in the anodic reaction must be consumed elsewhere on the steel surface to preserve electrical neutrality in the system. In other words, it is not possible for a large amount of electrical charge to build up at one location. Another chemical reaction must consume the electrons. Oxidation and reduction are coupled together as electrons are transferred between them. This reaction consumes both water and oxygen.

If the iron were simply to dissolve in the pore water, no cracking, delaminating, and spalling of the surrounding concrete would occur. Several more "downstream" reactions must occur for

corrosion products to form. This process can be expressed through the following steps. First, as shown in Equation 2.3, the products of the anodic reaction, Fe^{2+}, and the cathodic reaction, OH^-, react, producing ferrous hydroxide, $Fe(OH)_2$.

$$Fe^{2+} + 2OH^- \rightarrow Fe(OH)_2 \quad (2.3)$$

In Equation 2.4, ferrous hydroxide, $Fe(OH)_2$, is further oxidized to form ferric hydroxide, $Fe(OH)_3$.

$$4Fe(OH)_2 + O_2 + 2H_2O \rightarrow 4Fe(OH)_3 \quad (2.4)$$

As a result of dehydration (from exposure to the environment), Equation 2.5 shows how ferric hydroxide becomes ferric oxide, Fe_2O_3, commonly referred to as rust.

$$2Fe(OH)_3 \rightarrow Fe_2O_3 \cdot H_2O + 2H_2O \quad (2.5)$$

Dehydrated ferric oxide, Fe_2O_3, has a volume approximately twice that of the original steel reinforcement it replaces. When it becomes hydrated, ferric oxide swells even more and becomes porous, resulting in an increase in volume that could be two to ten times that of the original steel reinforcement volume. This expansion leads to cracking, delamination, and finally spalling of the concrete surrounding the reinforcing bars.

The electrical current flow resulting from the above process and the generation and consumption of electrons in the anode and cathode reactions are used in macrocell and half-cell potential measurements to assess corrosion activity. Interestingly, the fact that the anodic and cathodic reactions must balance each other for corrosion to proceed is the reason that epoxy coatings are believed to protect steel reinforcement.

2.2. Methods of Corrosion Monitoring

Techniques for corrosion monitoring are well established for RC structures. Because corrosion is an electrochemical process, the collection and interpretation of data is relatively easy. As introduced during the corrosion of steel reinforcement, electrons are released as a product of the anode chemical reaction. The electrons flow from the site of corrosion (anode) to a non-corroding site (cathode). This allows for corrosion risk and corrosion rate to be evaluated through electronic means (i.e., voltmeter measurements). Among the many possible techniques for corrosion monitoring, four techniques were used in the present study. For the sake of reference, each of these four techniques is described in the following sections.

2.2.1. Half-Cell Potential Monitoring

The corrosion risk of any steel reinforcement can be measured using the saturated calomel reference electrode shown in Figure 2.2. By placing the electrode on the concrete surface and connecting it via a voltmeter directly to the top or bottom reinforcement, a current is made to flow, and voltage is measured. The electrical potential difference (voltage) is known to be a

function of the iron in the pore water environment. As such, the electric potential is a measurement of the corrosion risk.

2.2.2. Macrocell Corrosion Monitoring

In the case of chloride attack, the anodes and cathodes (i.e., the corrosion locations) are often separated by areas of non-corroded steel. This is known as the macrocell phenomenon. In macrocell corrosion in bridge decks, the anode and cathode are commonly located on different steel bars, often the top and bottom layers.

Chloride-induced corrosion, the typical type of corrosion that occurs in bridge decks, is particularly prone to macrocell formation, as a high level of water is usually present to carry chloride ions into the concrete. The presence of water in the pores increases the electrical conductivity of the concrete. The higher conductivity allows the separation of the anode and cathode, as the chloride ions can easily transport through the water filled pores.

In North America, the macrocell is commonly used as a way of measuring the corrosion rate. The current flow between the top and bottom steel reinforcement layers is monitored by measuring the voltage across a resistor connecting the layers of reinforcement, as illustrated in Figure 2.3. By Faraday's Law, the mass loss rate (i.e., corrosion rate) is directly proportional to the monitored corrosion current.

2.2.3. CMS V2000 Silver-Silver Chloride Electrode Monitoring

With the CMS V2000 silver-silver chloride electrode (V2000 electrode), the potential difference between the silver electrode and the anode steel reinforcement is measured. This relationship is described by Faraday's laws and is a direct result of the relationship between dissimilar metals in the presence of an acidic or alkaline substance.

The electrochemical process of corrosion causes current via the flow of free electrons. The V2000 electrode generates a second, independent current as a function of the dissimilarity of the metals, the amount of moisture and chlorides present, etc. The two processes are additive.

By measuring both the induced voltage and current, the corrosion risk and corrosion rate can be determined. This makes the V2000 electrode a viable, permanent embedded sensor for the long-term monitoring of bridge deck steel reinforcement.

2.2.4. Chloride Ion Concentration Monitoring

The chloride concentration in concrete at the level of the reinforcement is a major factor in the corrosion of reinforcing steel. The chloride ions migrate to the reinforcement by permeating through the concrete or by penetrating through cracks in the concrete. To initiate the corrosion of steel reinforcement, the concentration of chloride ions must reach the previously described corrosion threshold at the steel reinforcement level.

The chloride ion concentration of concrete can be evaluated using several different methods. The AASHTO T 260-94 test (Sampling and Testing for Chloride-ion in Concrete and Concrete Raw

Materials) suggests three procedures (Procedure A, B, and C) for determining the chloride ion content in concrete (Scannell and Sohanghpurwala 1996). Procedures A and B are time consuming and complicated tests: Procedure A determines the chloride ion concentration potentiometric titration, whereas Procedure B uses an atomic absorption process to determine the concentration of chloride ion. In Procedure C, the chloride ion concentration is determined using a specific ion probe.

An alternative to these three procedures is the nondestructive use of X-ray fluorescence (XRF) spectroscopy to analyze the chloride ion concentration in the powder samples. XRF spectroscopy provides an analytical means to identify and quantify the concentration of elements contained in a solid, powdered, and liquid sample (Schlorholtz 1998).

(a) Saturated calomel reference electrode

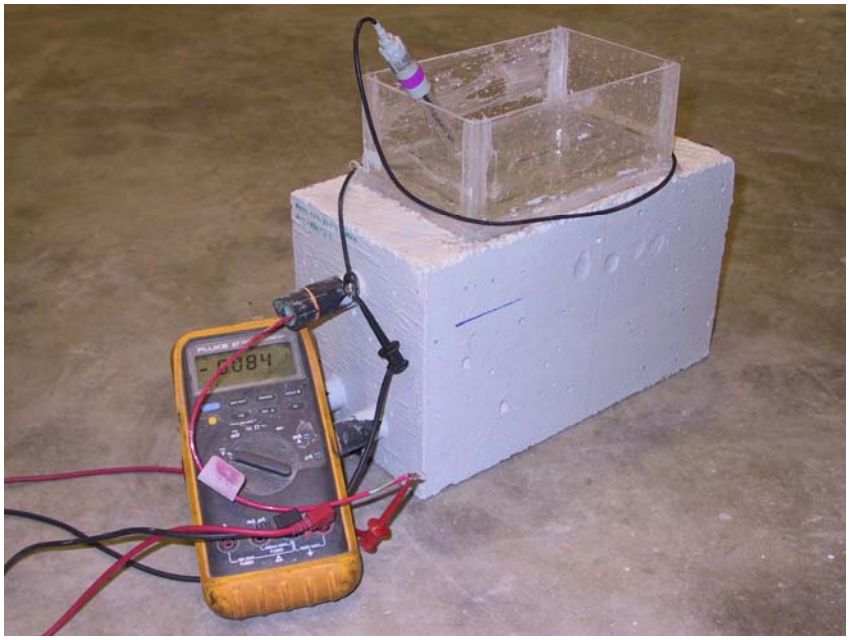

(b) Measure of half-cell corrosion potential for the top layer of reinforcement

Figure 2.2. Half-cell corrosion potential monitoring method

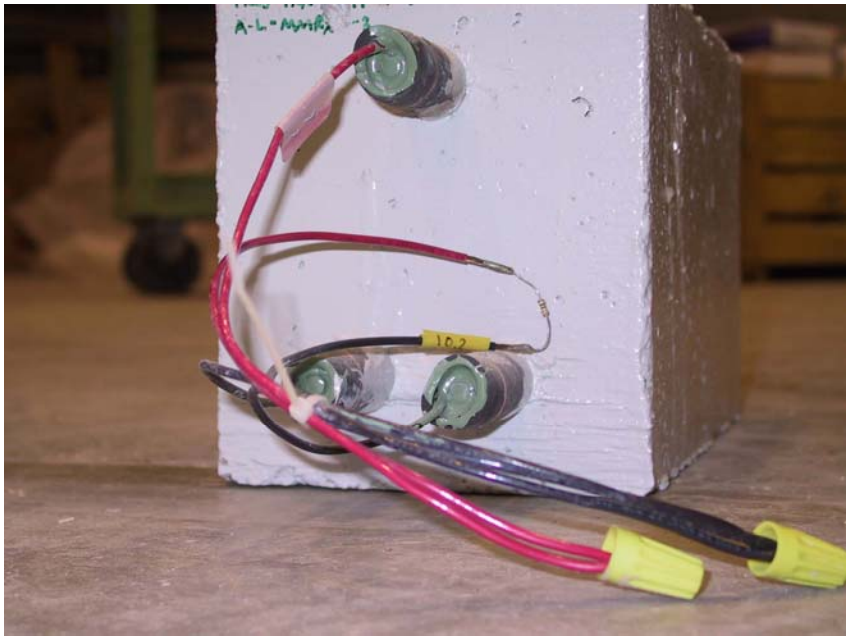

(a) Top and bottom reinforcement layers connected via resistor

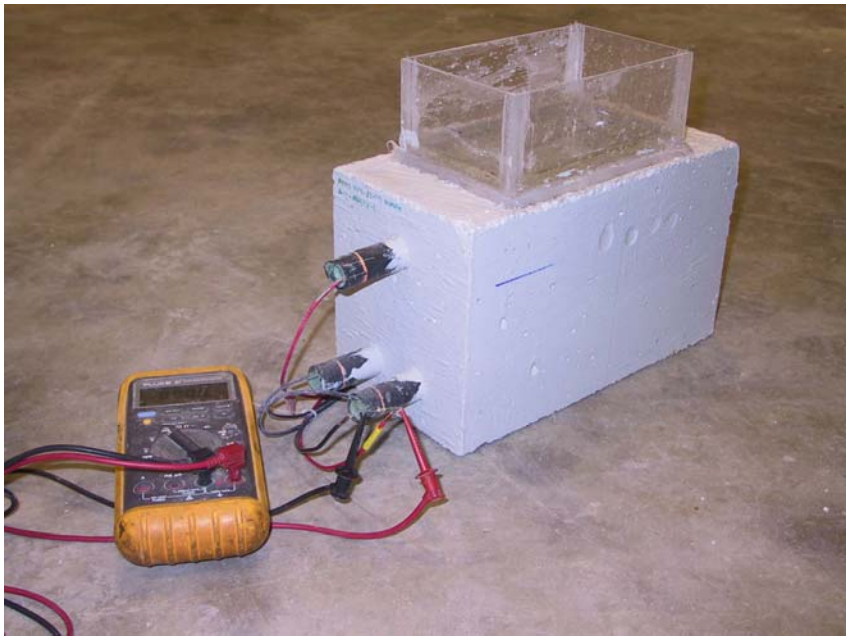

(b) Measurement of macrocell corrosion

Figure 2.3. Macrocell corrosion monitoring method

Figure 2.4. CMS V2000 silver-silver chloride electrode

2.3. MMFX Microcomposite Steel Reinforcement Research

MMFX microcomposite steel reinforcement is publicized as a proprietary chemical composition material and advertised as having a unique microstructure with enhanced corrosion resistance characteristics and higher mechanical properties (yield and tensile strengths) than conventional ASTM A 615 steel.

With no published study available concerning MMFX reinforcement performance, the University of Kansas Center for Research conducted a study to evaluate the performance of MMFX reinforcement, with a major emphasis placed on comparing the corrosion resistance of MMFX, epoxy-coated reinforcement, and uncoated reinforcement (Darwin et al. 2002). This study was conducted in cooperation with the United States Department of Transportation (DOT), the FHWA, the Kansas DOT, the South Dakota DOT, and the National Science Foundation. The Rapid Macrocell accelerated corrosion test was used as the principal evaluation test in that study. The complete evaluation involved corrosion testing, measurement of bar deformation, analysis of material composition, and a general study of the impact of the material's reinforcement properties on the structural performance of bridge decks. The results of the laboratory evaluation were supplemented with construction and maintenance experience in South Dakota and other states to evaluate the impact of implementing MMFX on the life expectancy and cost effectiveness of concrete bridge decks.

From the physical and mechanical tests conducted by the University of Kansas Center for Research, several issues in implementing MMFX reinforcement were identified in three sample bridge deck designs in South Dakota. Based only on design, MMFX reinforcement provides few satisfactory options for replacing conventional reinforcement under the current AASHTO design procedures. For example, MMFX reinforcement was found to exceed the maximum allowable

steel and concrete stresses, violate crack control and fatigue provisions, and exceed the maximum allowable percentage of reinforcement (Darwin et al. 2002). Furthermore, the mechanical properties provided by the manufacturer were found to be higher than the properties described by a series of tests conducted by the University of Kansas Center for Research, shown in Table 2.1 (MMFX Steel Corporation of America 2003; Darwin et al. 2002). From laboratory corrosion testing, epoxy-coated reinforcement was found to be more effective in corrosion resistance than the MMFX steel. Overall, the report concluded that using MMFX reinforcing steel in bridge decks did not appear to be cost effective compared to using epoxy-coated reinforcement.

Table 2.1. Mechanical properties of MMFX Microcomposite steel reinforcement

Given by	Yield strength, MPa (ksi)	Tensile strength, MPa (ksi)
MMFX Steel Corporation of America	0.820–0.916 (119–133)	1.240–1.281 (180–186)
Kansas Department of Transportation	0.758–0.827 (110–120)	1.102–1.206 (160–175)

This primary conclusion met with some criticism from the manufacturer of MMFX reinforcement. The MMFX Steel Corporation of America submitted a critique of the laboratory evaluation conducted by the University of Kansas Center for Research, presenting concerns to be addressed in future research. The study presented herein will attempt to incorporate these issues through the following means:

- The principle differences between the cracked beam accelerated corrosion test and the ASTM G 109 accelerated corrosion test are that (1) the cracked beam specimens used by the University of Kansas Center for Research allow a higher concentration of chlorides (i.e., 15% sodium chloride) direct access to the top layer of reinforcement through a fabricated crack and (2) a “severe” drying regime uses an elevated temperature. While the general ASTM G 109 specimen does not employ a fabricated crack, as did the specimen used by the University of Kansas Center for Research, the present study will similarly use a cracked specimen to accelerate the diffusion of chloride ions through the concrete. However, beyond fabricating a crack, the present study uses the lower chloride concentration (3% sodium chloride) and the non-heat drying regimen of the ASTM G 109 accelerated corrosion test.
- For the Rapid Macrocell accelerated corrosion test developed by the University of Kansas Center for Research, the MMFX Steel Corporation suggested that, to establish realistic corrosion rates, the test could be improved by embedding the cathode in greater concrete cover. To accommodate this recommendation for the present study, the forms in which the specimens were cast were increased from the 38 mm (1.5 in.) diameter PVC pipe used by the University of Kansas Center for Research to a 76 mm (3 in.) diameter PVC pipe.
- Determining chloride threshold concentrations from a laboratory test in which the rate of chloride ingress is greatly accelerated is problematic because the chloride ion concentration at the level of steel reinforcement may be much higher than the threshold when corrosion activity is first detected by periodic monitoring. While periodic monitoring will give rise to uncertainty, using the lower chloride concentration outlined by ASTM G 109, will minimize the change in chloride ion concentration between

successive measurements.

- The chloride exposure conditions performed by the University of Kansas Center for Research are believed to produce higher corrosion rates than those produced in field conditions. As previously discussed, to alleviate the uncertainty associated with the higher chloride concentration used by the University of Kansas Center for Research, the present study decreased the chloride concentration to that outlined by ASTM G 109.
- None of the epoxy-coated reinforcement corrosion data collected by the University of Kansas Center for Research were used in the life expectancy and cost effectiveness analyses. The researchers instead relied solely on the field performance of epoxy-coated reinforcement. In contrast, the life expectancy presented for each reinforcement type tested in the present study was calculated based on measured laboratory chloride ion concentrations, corrosion initiation, and corrosion rate for each reinforcement type.

PART I: FIELD EVALUATION

3. BRIDGE AND CORROSION MONITORING SYSTEM DESCRIPTION

This chapter describes the physical characteristics of the two newly constructed bridges evaluated in this study. The layout and installation of corrosion sensors and the monitoring protocols followed are also described.

3.1. Construction and Description of Bridge

The subject bridges are new twin 83.5 m x 12 m (274 ft. x 39.37 ft.) three-span, pre-stressed concrete girder bridges constructed in 2002. The bridges are located in northeast Iowa on relocated US 20 over South Beaver Creek in Grundy County, Iowa. The bridges have a total length of 83.5 m (274 ft.) consisting of two 24.75 m (81.20 ft.) end spans and a 34 m (111.55 ft.) center span. The bridge deck is a nominal 200 mm (7.87 in.) thick, cast-in-place reinforced concrete slab that includes a 13 mm (0.51 in.) integral wearing surface. The roadway width is 12 m (39.37 ft.), allowing two traffic lanes with a narrow shoulder on each side. The decks of the two bridges were constructed with two different types of reinforcing steel: MMFX steel in the eastbound bridge (referred to as MMFX bridge) and epoxy-coated steel in the westbound bridge (referred to as epoxy bridge). There was essentially no difference in how these two bridges were constructed. The top transverse reinforcing steel was placed parallel to and 65 mm (2.56 in.) (clear) below the top of the slab, while the bottom transverse reinforcing steel was placed parallel to and 25 mm (0.98 in.) (clear) above the bottom of the slab. The deck is supported by six pre-stressed concrete beams spaced at 2,200 mm (86.61 in.) on center. All slab and diaphragm reinforcing steels were tied in place and adequately supported before concrete was poured. In all cases, the pier and abutment diaphragm concrete was placed monolithically with the floor slab. Moderate curbs were constructed integrally with the deck, and concrete guardrails were connected to the curbs. The concrete decks were cast for both bridge decks in May 2002 and were opened to traffic in August 2003. See Figure 3.1 for a general framing plan and typical cross-section of the subject bridges. In addition, typical photographs of the subject bridges taken during construction are shown in Figures 3.2 through 3.6.

3.2. Corrosion Monitoring System

Corrosion detecting devices installed on both bridge decks consisted of the V2000 monitoring electrodes described above (see Figure 2.4). These sensors consist of a solid silver-silver chloride wire electrode wrapped in a permeable, non-conducting PVC covering. These are used to monitor reinforcing steel in concrete for the onset of corrosion, cessation of corrosion, and intensity of corrosion growth.

The use of this embeddable sensor offers the ability to monitor the interior state of a structure by measuring parameters that can be used as reliable indicators of the likelihood of corrosion in the surrounding area. Although the sensors do not address the specific electrochemical mechanisms, they provide a reliable and cost-effective monitoring system to measure the basic electrochemical processes.

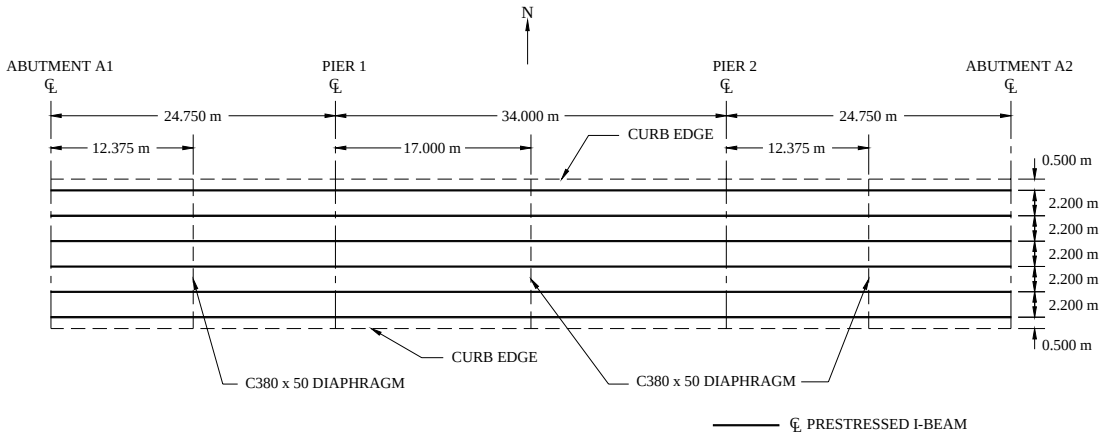

(a) General framing plan

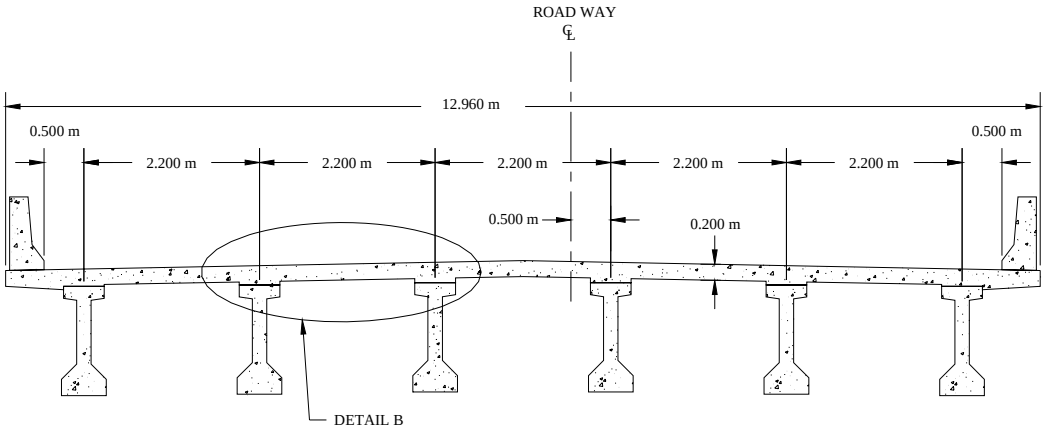

(b) Typical cross-section

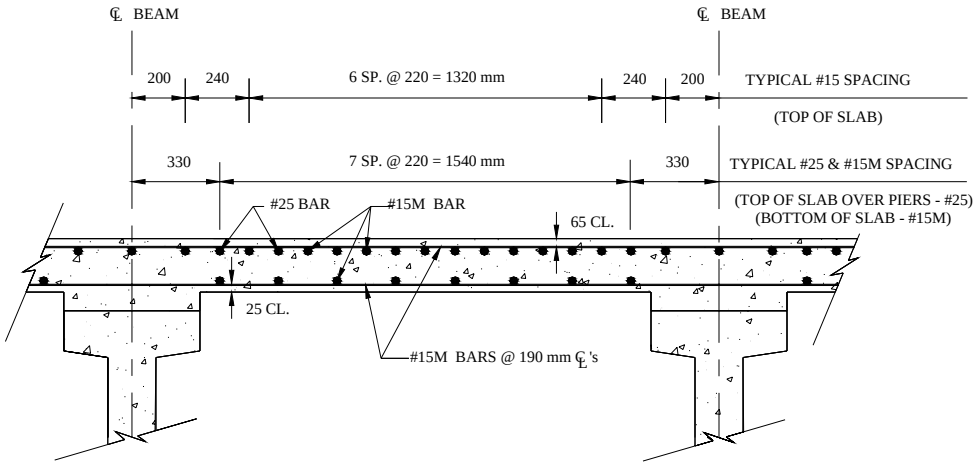

(c) Detail B

Figure 3.1. Bridge framing plan and typical cross-section

(a) Typical beam layout

(b) Side view

(c) Typical beam connection at pier

Figure 3.2. Typical prestressed I-beams

Figure 3.3. Typical end view

(a) MMFX bridge (looking northwest)

(b) MMFX bridge (looking west)

(c) Epoxy bridge (looking southwest)

(d) Epoxy bridge (looking west)

Figure 3.4. Bridge deck concrete placement

Figure 3.5. Bridge deck concrete placement completed

(a) Side view (MMFX bridge)

(b) Side view (Epoxy bridge)

(c) End view

(d) Bottom view (abutment)

(e) Bottom view (center span and west pier)

Figure 3.6. Completed bridge

Both bridges were instrumented with V2000 electrode sensors permanently embedded in the concrete deck. Figure 3.7 shows a plan view with the sensor locations, with "detail C" given in Figure 3.8. A total of twenty No. 25 top bars were instrumented (10 on each bridge: M1 through M10 on MMFX bridge, and E1 through E10 on epoxy bridge) in the negative bending moment region near the eastern drainage points. The sensors were wound around a length of approximately 4.6 m (15.09 ft.) of each bar. Each electrode was connected to a red lead wire with a protected butt splice (see Figure 3.9). A black wire was attached directly to the bar using a stainless steel clamp. These lead wires (see Figure 3.10), run out of the deck, are used to measure the internal voltage and electrical current.

On the epoxy bridge, two additional short sections of MMFX bars were instrumented with electrodes and placed between other epoxy coated bars (i.e., one on the north side, referred to as "NO," and one on the south side, referred to as "SO") to compare the two types of bars in exactly the same environment. Figures 3.11 and 3.12 show typical photographs of the instrumentation layout.

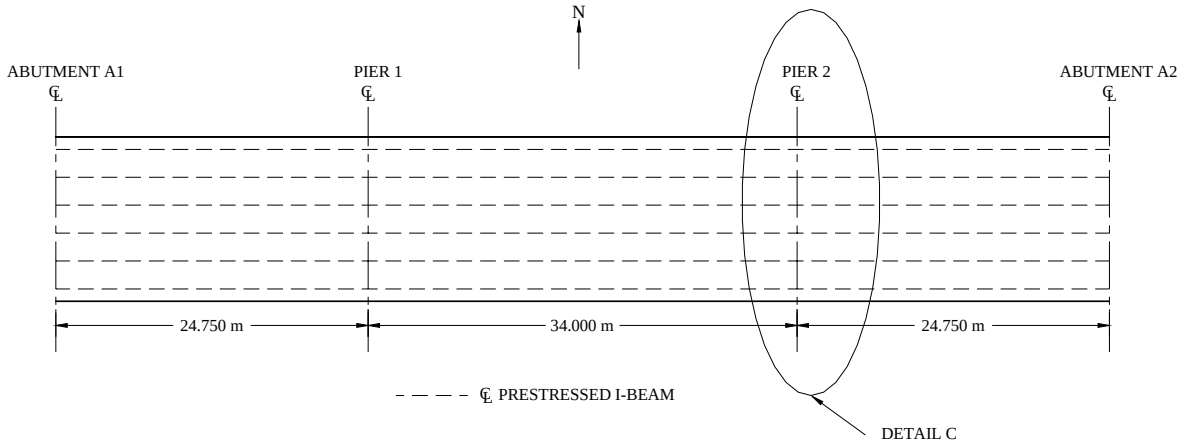

Figure 3.7. Plan view with sensor location

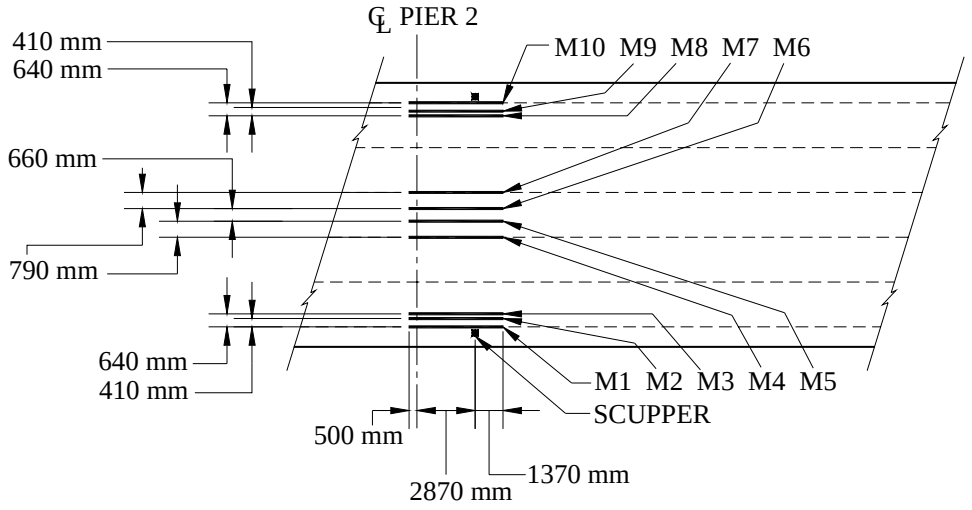

(a) MMFX bridge

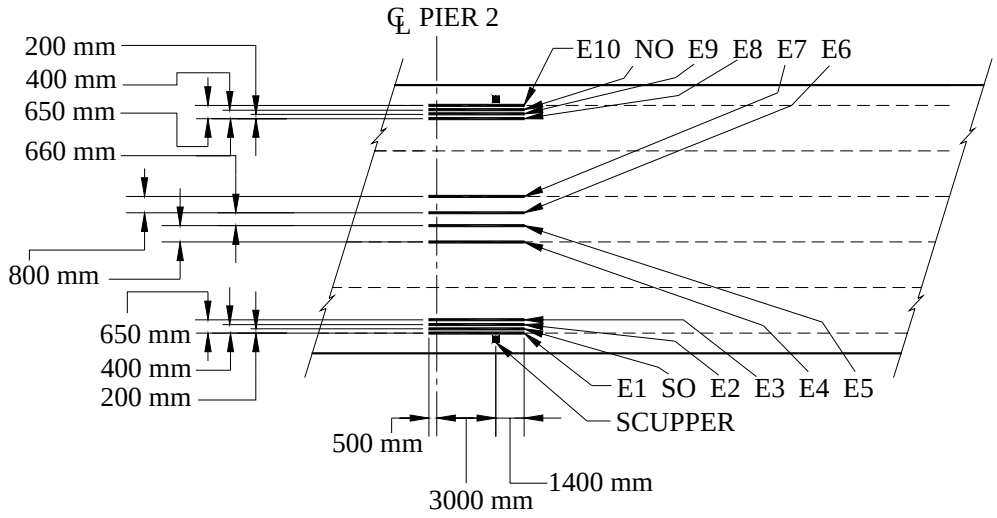

(b) Epoxy bridge

Figure 3.8. Detail C (general instrumentation of V2000 sensors)

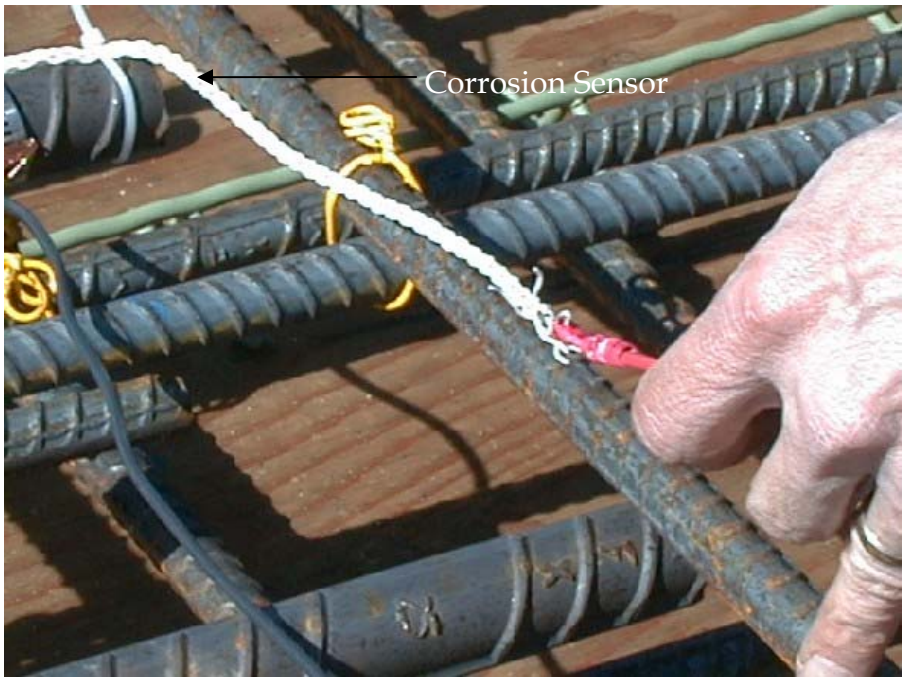

(a) Butt splice of electrode corrosion sensor and lead wire

(b) Butt splice protected with butyl rubber underneath aluminum foil tape

Figure 3.9. Connecting V2000 sensor with lead wire

Figure 3.10. Extending lead wires for data measurement

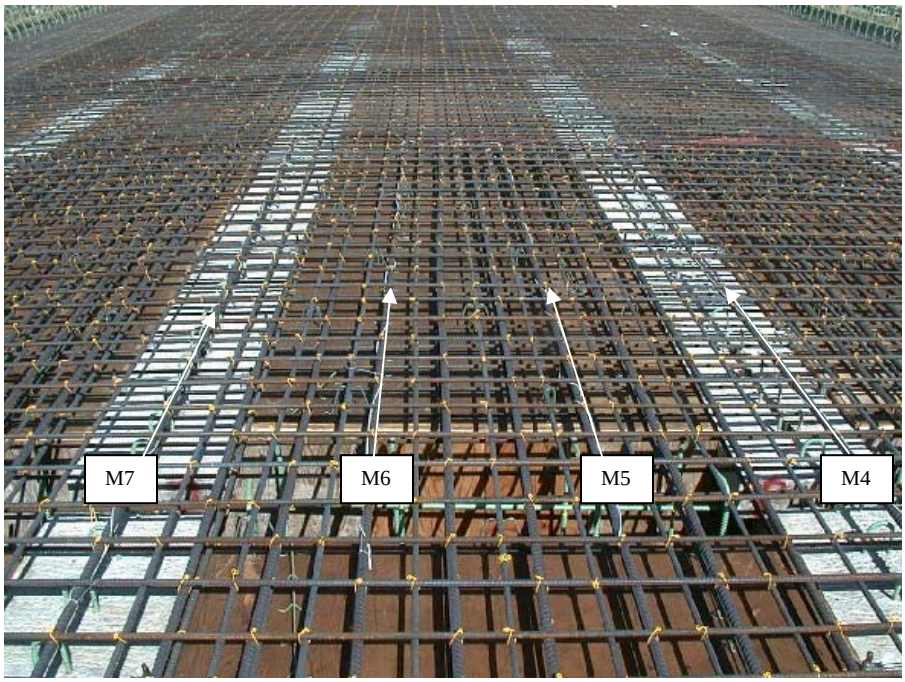

Figure 3.11. Typical instrumentation layout on MMFX bridge

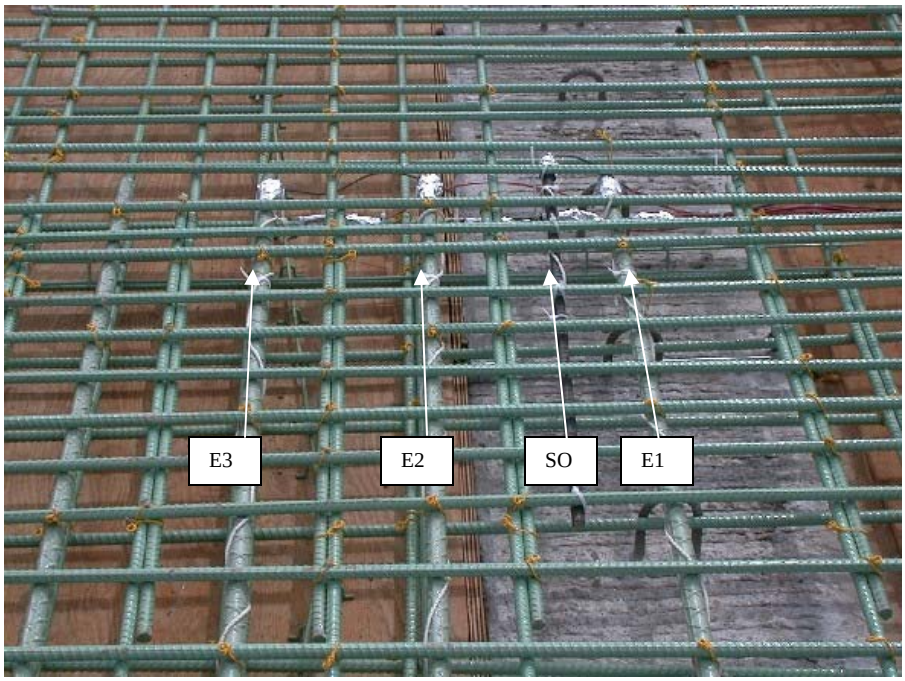

(a) "SO" MMFX bar and epoxy bars E1–E3 (looking east)

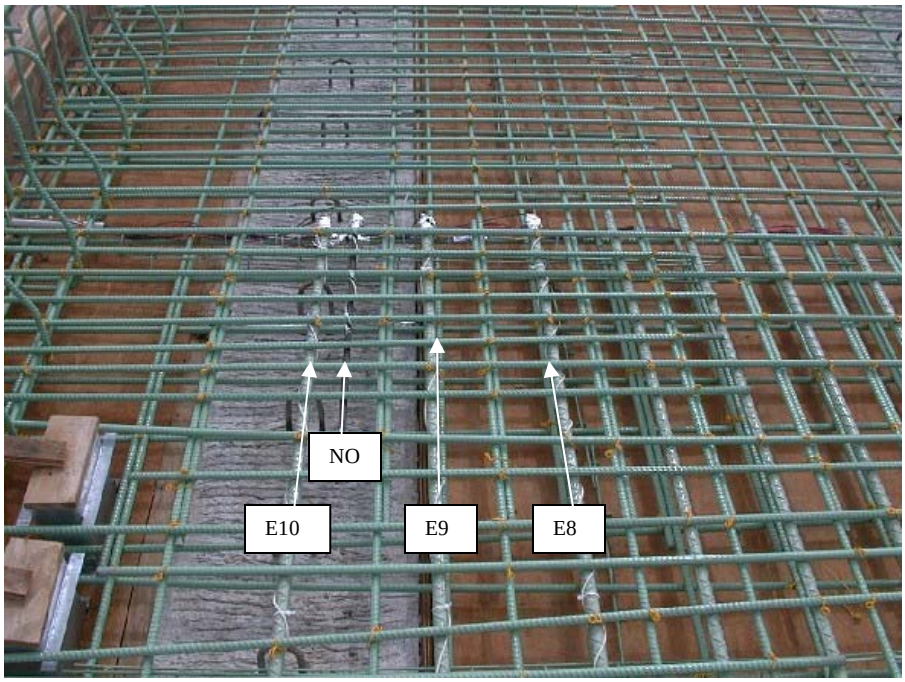

(b) "NO" MMFX bar and epoxy bars E8–E10 (looking east)

Figure 3.12. Typical photographs of the instrumentation layout on epoxy bridge

3.2.1. Monitoring Concept

The electrical process induced by steel cathode corrosion is an electrochemical process, as discussed abbove. An electric potential difference arises when the electrochemical reaction takes place. With the V2000 electrode, the potential between the electrode sensor and the bar is measured. In this case, the electrode sensor serves as the cathode and the rebar as the anode, thereby creating a "battery." The electrochemical process, on the other hand, is separate and distinct from the battery formed by the V2000 electrode cable (silver-silver chloride), steel, and alkaline concrete. This electrochemical reaction occurs when a local pH value at the concrete-steel interface drops below nine due to an incursion of chlorine atoms. During this process, electrons are released as a product of the chemical reaction. Therefore, the corrosion site acts as another independent "chemical battery." These two batteries then become additive to one another, and the internal voltage increases. By measuring DC voltage and DC current with a voltmeter (see Figure 3.13), the corrosion activity occurring on each bar and the corrosion's severity can be determined.

The actual output value depends primarily on the conditions of the concrete after placement. It is normal to expect high voltage levels (possibly over 1000 mV) shortly after concrete placement, since considerable moisture is present. While the concrete is fresh and uncured, it is highly active and generates a high output. As the concrete cures, this initial spike typically subsides to within the "normal" range of less than 400 mV.

In general, electrical current readings below 0.100 mA (1000 μA) can be considered a weak site of corrosion. When corrosion occurs, however, a natural DC current starts to flow from one area to another, and the electrical current increases significantly; if it exceeds 1000 μA, corrosion activity is considered quite active.

Figure 3.13. Data measuring with voltmeter

4. FIELD MONITORING AND DISCUSSION

Visual inspections of both bridges have been conducted regularly to identify any signs of corrosion. As of November 2005, no obvious external signs of damage have been observed.

Figures 4.1 and 4.2 show the internal voltage and current readings for all instrumented reinforcing bars in both bridge decks as of November 2005. All MMFX bridge data appear to be as expected; although the voltage data increased above 400 mV (see Figure 4.1a) at the initial stage, the voltage returned to normal levels after concrete cure (i.e., the initial spike has ceased). Note that, even at this initial stage, the electrical current remained below 1000 μA (indicative of a weak corrosion site), as shown in Figure 4.2a. After approximately three months, all voltage levels for the MMFX bridge dropped steadily and remained within the normal range, at less than 100 mV. At this time, it appears that there is no ongoing corrosion activity.

The epoxy-coated bars, on the other hand, behaved somewhat unexpectedly. Readings on the epoxy bridge were higher than originally expected (about two times higher than the readings on the MMFX bridge). During the initial stage, shortly after concrete placement, some readings increased over 1,200 mV (see Figure 4.1b). Although these high data readings dropped below 400 mV, some of the readings (E2, E4, and E10) are still above or close to 200 mV. Theoretically, there should be near-zero readings if the bars are coated perfectly; the steel would be perfectly protected with no contact between the steel and the concrete. As shown in Figures 4.1b and 4.2b, however, it is speculated that contact has been made on some of the bars being monitored. This indicates that there are at least one or more defects (i.e., coatings may have been nicked and/or scratched during construction) in the epoxy coating on some bars.

Note that some data show negative readings (M8 and SO). This is attributed to the possibility that the lead wires were either connected in reverse or damaged during concrete placement.

Overall, the data indicate that readings are lower on the MMFX bridge than on the epoxy bridge. Some of the bars (E2, E4, and E10) need to be closely monitored in the future, since they showed relatively high readings. It should be noted, however, that no significant active corrosion is observed in either bridge deck at this point, as shown in Figure 4.2. It is the authors' opinion that, with monitoring and evaluation of further data, this investigation will allow engineers to better understand the performance of these reinforcing steels under actual service conditions.

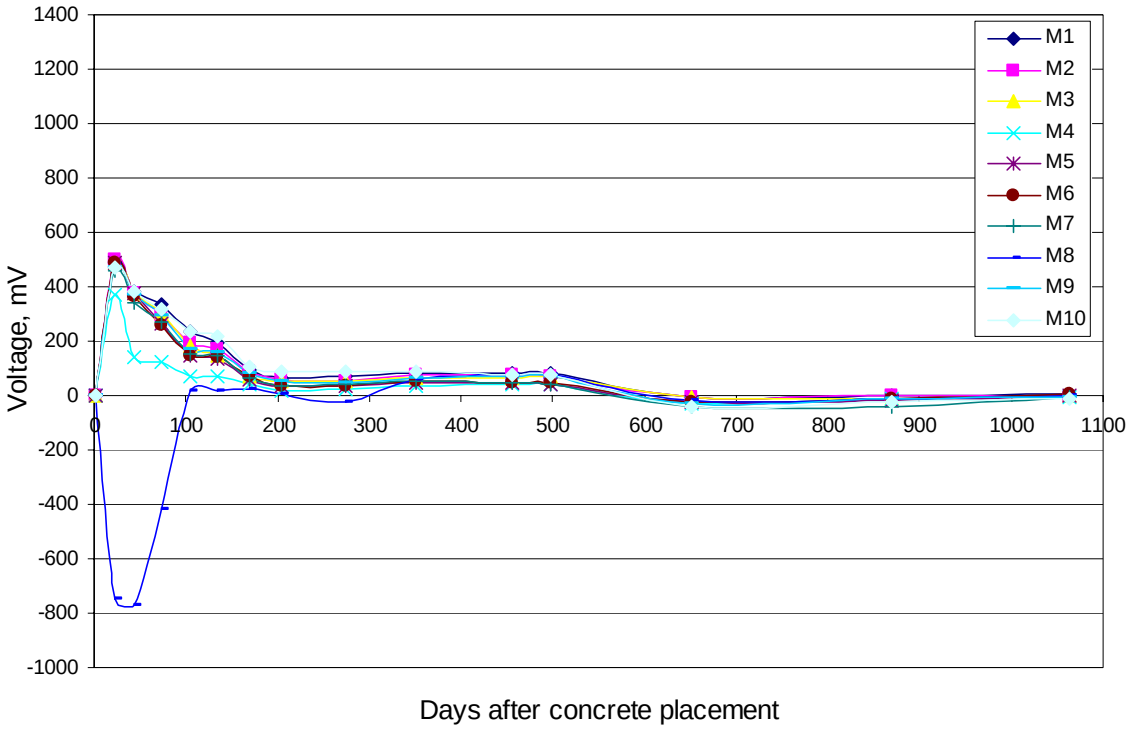

(a) MMFX bridge

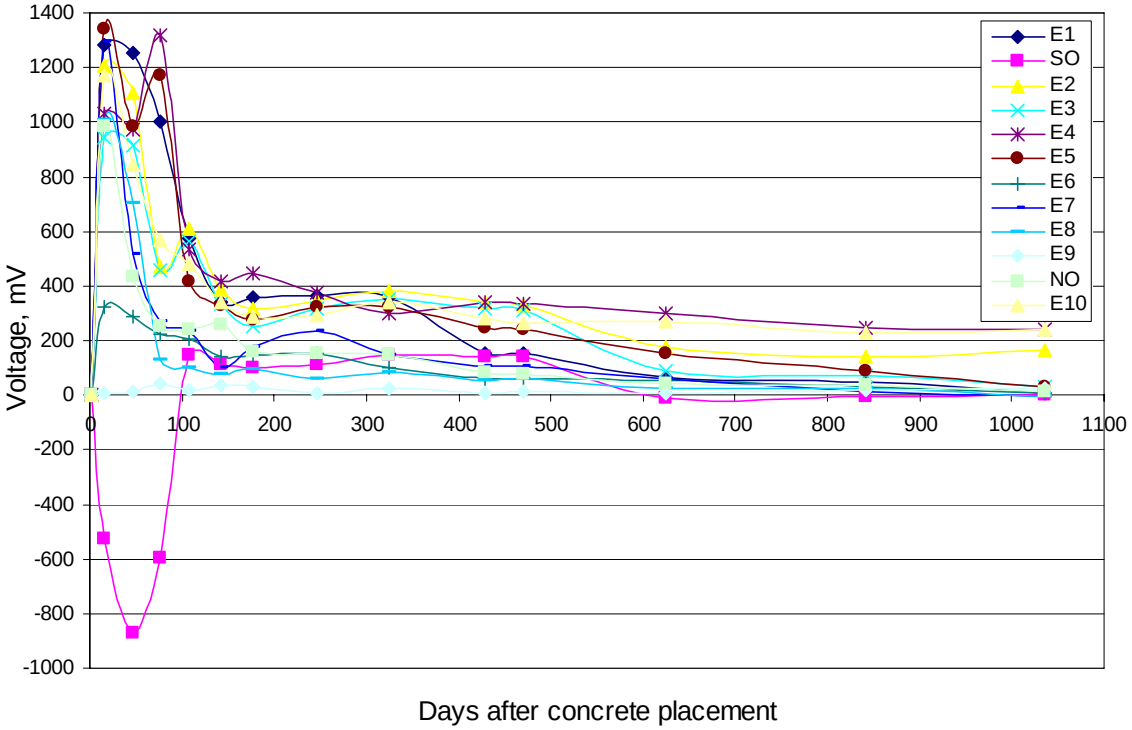

(b) Epoxy bridge

Figure 4.1. Voltage readings from V2000 sensors on instrumented reinforcing bars

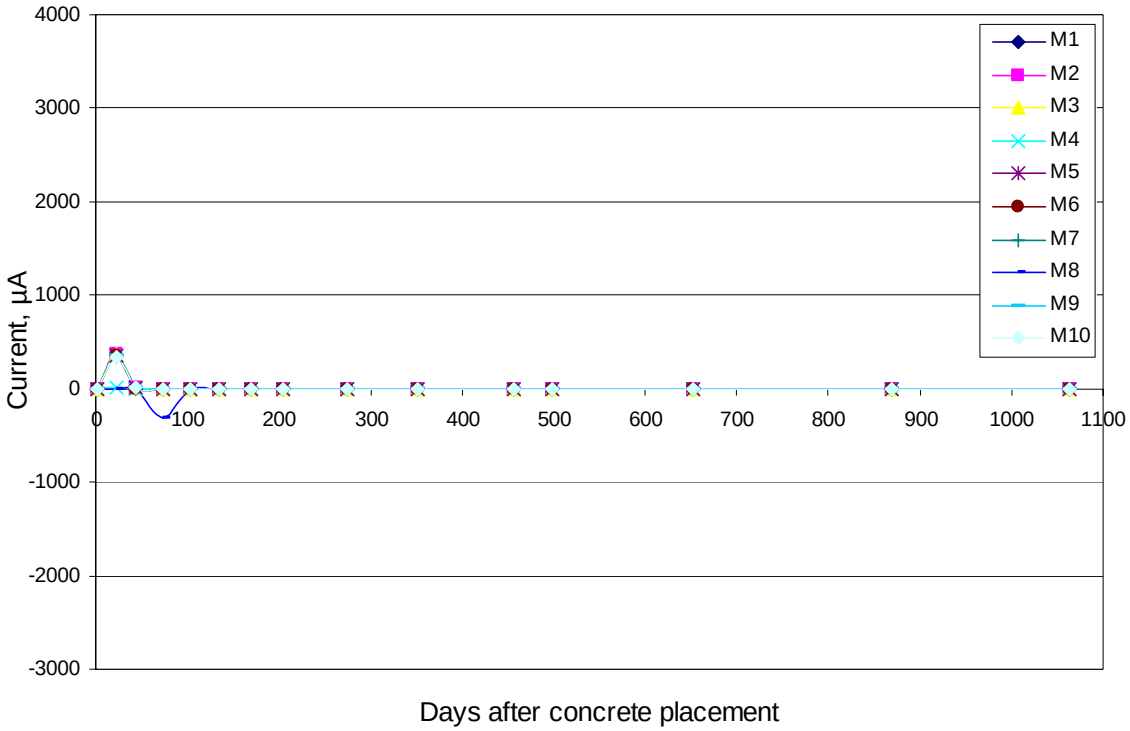

(a) MMFX bridge

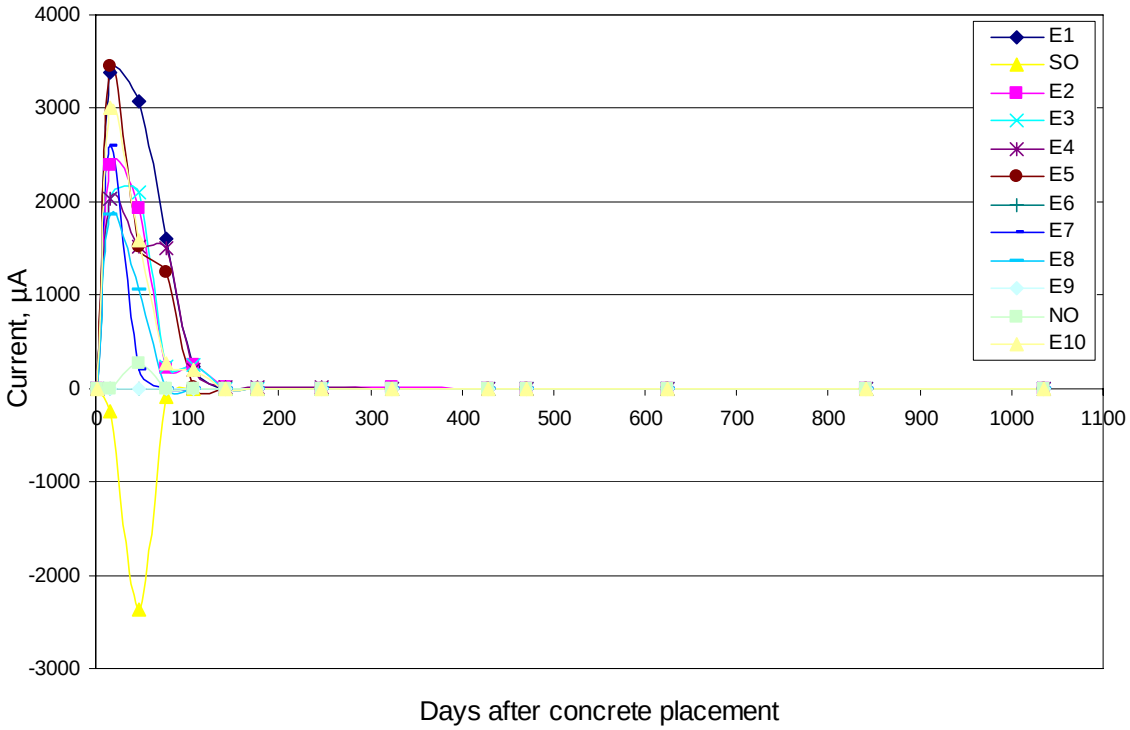

(b) Epoxy bridge

Figure 4.2. Current readings from V2000 sensors on instrumented reinforcing bars

PART II: LABORATORY EVALUATION

5. LABORATORY TEST DESCRIPTION

As previously stated, the principal reason for selecting a new reinforcement material for concrete bridge decks is to improve the life expectancy and cost effectiveness of the structural system. A feature of the material, which presumably is more expensive, is that it provides an improvement in corrosion resistance compared to the current material of choice, epoxy-coated mild steel reinforcement, while at the same time meeting the requirements of ASTM A 775. In light of this requirement, the following portion of the study compared the corrosion resistance of MMFX microcomposite steel reinforcement with that of epoxy-coated and uncoated mild steel reinforcement using the ASTM G 109 accelerated corrosion laboratory test. An additional test method introduced by the University of Kansas Center for Research, referred to as the Rapid Macrocell accelerated corrosion test, was also used for this evaluation.

5.1. Material Properties

Steel reinforcement used in the laboratory test program described below consisted of one heat each of No. 16 (No.5) MMFX, epoxy-coated reinforcement, and uncoated reinforcement. The MMFX reinforcement was obtained from the Iowa DOT and is the same material used in the field bridge described in Part I. The epoxy-coated reinforcement was provided for evaluation by Construction Material Incorporated of Des Moines, Iowa. The uncoated reinforcement was acquired through a local distributor. In the specimens described subsequently, a single batch of concrete was utilized to preserve uniformity among the individual test specimens and between the tests. The following paragraphs describe the properties of the materials used in the subsequently described corrosion monitoring tests.

5.1.1. Steel Reinforcement Properties

Although published data exist, the MMFX, epoxy-coated reinforcement, and uncoated reinforcement used in the laboratory study were tested to determine yield strength, tensile strength, and elongation. Three specimens of each steel type were tested to determine the mechanical properties following ASTM E8.

The results of the mechanical tests are presented in Table 5.1. Yield strengths were measured based on a well-defined yield point for the epoxy-coated and uncoated steels and were based on the 0.2% offset method for the MMFX steel. Data are reported for No. 16 (No. 5) MMFX, epoxy-coated reinforcement, and uncoated mild reinforcement with the as-delivered cross-sections. The average of the three trials per reinforcement type is also reported.

The No. 16 (No. 5) MMFX reinforcement exhibited yield strengths between 0.787 and 0.816 MPa (114.2 and 118.4 ksi), with an average of 0.787 MPa (114 ksi). Tensile strengths were recorded between 1.089 and 1.154 MPa (158.0 and 167.5 ksi), with an average of 1.127 MPa (163 ksi). The total elongations at failure ranged between 6.9% and 7.5%, with an average of 7.2%.

Table 5.1. Mechanical properties of steel reinforcement

Reinforcement identification	Yield strength, MPa (ksi)	Tensile strength, MPa (ksi)	Elongation, percent in 0.61 m (24 in.)
MMFX[1] (1)	0.787 (114.2)	1.138 (165.1)	7.5
MMFX (2)	0.762 (110.6)	1.089 (158.0)	7.3
MMFX (3)	0.816 (118.4)	1.154 (167.5)	6.9
MMFX Average	*0.788 (114.4)*	*1.127 (163.5)*	*7.2*
UC[2] (1)	0.403 (58.5)	0.661 (96.0)	16.4
UC (2)	0.414 (60.1)	0.661 (96.0)	16.6
UC (3)	0.414 (60.1)	0.659 (95.6)	16.2
UC Average	*0.411 (59.6)*	*0.661 (95.9)*	*16.4*
EC[3] (1)	0.460 (66.7)	0.744 (106.6)	14.3
EC (2)	0.462 (67.1)	0.732 (106.3)	13.5
EC (3)	0.453 (65.7)	0.717 (104.1)	9.8
EC Average	*0.458 (66.5)*	*0.728 (105.7)*	*12.6*

1 MMFX – MMFX Microcomposite steel reinforcement

2 UC – Uncoated mild steel reinforcement

3 EC – Epoxy-coated mild steel reinforcement

These values match those obtained by the University of Kansas Center for Research and differ from those reported by the MMFX Steel Corporation of America given in Table 2.1. The University of Kansas Center for Research reported a yield strength range from 0.758 to 0.827 MPa (110 to 120 ksi), a tensile strength range from 1.102 to 1.206 MPa (160 to 175 ksi), and an elongation range from 6.3% to 7.8% (Darwin et al. 2002). Conversely, the MMFX Steel Corporation of America reported a yield strength range from 0.820 to 0.916 MPa (119 to 133 ksi) and a tensile strength range from 1.240 to 1.282 MPa (180 to 186 ksi) (MMFX Steel Corporation of America 2003).

Yield strengths for the No. 16 (No. 5) uncoated reinforcement ranged from a low of 0.403 MPa (58.5 ksi) to a high of 0.414 MPa (60.1 ksi), with an average of 0.411 MPa (59.6 ksi). Tensile strengths ranged from 0.659 to 0.661 MPa (95.6 to 96.0 ksi), with an average of 0.661 MPa (95.9 ksi). Elongations ranged from a low of 16.2% to a high of 16.6%, with an average of 16.4%.

The No. 16 (No. 5) epoxy-coated reinforcement exhibited yield strengths between 0.453 and 0.462 MPa (65.7 and 67.1 ksi), with an average of 0.458 MPa (66.5 ksi). Tensile strengths were recorded between 0.717 and 0.744 MPa (104.1 and 106.6 ksi), with an average of 0.728 MPa (105.7 ksi). The total elongations at failure ranged between 9.8% and 14.3%, with an average of 12.6%.

5.1.2. Concrete Mix Properties

All of the test specimens described in the following section were constructed from a single 1.5 cu. yd. batch of ready mix concrete to ensure that the MMFX, epoxy-coated steel, and uncoated steel reinforcement were subject to similar conditions. Compressive strength and modulus of rupture tests for the concrete were conducted and are summarized in Table 5.2, along with other

pertinent information.

Table 5.2. Mix proportions per cubic yard and concrete properties

Property	Quantity
Cement	227 kg (500 lb.)
Sand	692 kg (1,526 lb.)
Course aggregate[1]	675 kg (1,489 lb.)
Water	98 kg (217 lb.)
Fly ash	29 kg (64 lb.)
Air-entraining agent	56.7 g (2 oz.)
Air content	5.5%
Unit weight	2263 kg/m^3 (3,815 pcy)
Slump	7.62 cm (3.0 in.)
Average 28-day compressive strength	39.232 MPa (5,964 psi)
Average 28-day modulus of rupture	4.292 MPa (623 psi)

1 Course aggregate – 3/8 inch nominal maximum size

5.2. Accelerated Corrosion Test Program

Corrosion resistance performance is generally evaluated based on accelerating the corrosion process in laboratory specimens. Changes in corrosion potential, relative corrosion rates, and chloride concentrations needed for corrosion initiation are commonly monitored. In this study, interval powder samples were also collected and analyzed through X-ray fluorescence spectrometry for chloride content comparison.

5.2.1. Accelerated Corrosion Tests

Both the ASTM and Rapid Macrocell accelerated corrosion tests used in this study induce general and pitting corrosion and are generally believed to provide valid corrosion performance comparisons. The study described below used these two test methods to accelerate the corrosion of different types of steel embedded in concrete.

5.2.1.1. ASTM G 109 Accelerated Corrosion Test

The ASTM G 109 accelerated corrosion test (ACT) was the test first developed to study the effective corrosion protection of chemical admixtures on steel reinforcement (ASTM 2001). While the ASTM ACT was originally developed to evaluate admixture materials intended to inhibit chloride-induced corrosion of steel in concrete, over the past two decades the test method has been most notably used to evaluate the corrosion response of steel reinforcement. Although the ASTM ACT typically requires one to two years for completion, the test method provides a severe corrosion environment that is believed to simulate 30 to 40 years of exposure for bridges.

The ASTM ACT models the corrosion of steel reinforcement in concrete in which two layers of reinforcement are present (i.e., the test simulates the cross-section of a bridge deck). The test specimen consists of a small beam constructed with two layers of steel reinforcement. The top layer includes one bar, while the bottom layer includes two bars placed side-by-side. The layers are connected electrically by a 10 ohm resistor, and the sides of the concrete are sealed with epoxy. A reservoir is secured to the top of the beam to allow liquid to pool on the upper surface.

The test (illustrated in Figure 5.1) subjects 229 mm (9 in.) of reinforcement below the surface to alternating cycles of wetting and drying with a 3% sodium chloride solution. The cycles of wetting allow for chloride ingress into the reinforcement level, while the cycles of drying allow for oxygen to replenish.

The half-cell corrosion potentials for the top and bottom layers indicate the onset of corrosion. At the initiation of corrosion, concrete powder samples are taken at the level of the top reinforcement to estimate the chloride ion concentration required for corrosion initiation. The corrosion rates are determined by measuring the voltage drop across the resistor.

5.2.1.2. Rapid Macrocell Accelerated Corrosion Test

The Rapid Macrocell ACT was originally developed at the University of Kansas under the Strategic Highway Research Program (SHRP) (Chappelow et al. 1992; Martinez et al. 1990) and updated under the National Cooperative Highway Research Program-Innovations Deserving Exploratory Analysis (NCHRP-IDEA) (Darwin et al. 2002). The goal of the test is to obtain a realistic measure of the performance of corrosion protection systems over a shorter period of time than traditional ACTs, such as the ASTM ACT.

The basic test system requires two containers and consists of either bare or mortar-clad steel reinforcement. This system is illustrated in Figure 5.2. The contact surface between the mortar and the bar simulates the concrete-reinforcement interface in actual structures. A single bar, either bare or mortar-clad, is placed in a 1 qt. container with a simulated pore solution containing a 3% concentration of sodium chloride. Two bars are placed in a second 5 qt. container and immersed in simulated pore solution with no chlorides added. The solution in both containers submerges 76 mm (3 in.) of reinforcement below the solution surface. The solutions in the two containers are connected by a salt bridge, and the test specimen in the pore solution containing sodium chloride (anode) is electrically connected through a single 10 ohm resistor to the two specimens in the simulated pore solution (cathode).

Air is bubbled into the pore solution surrounding the cathode to ensure that an adequate supply of oxygen is present for the cathodic reaction. The air causes some evaporation, which is countered by adding distilled water to this container to maintain a constant solution volume.

Similar to the ASTM ACT, half-cell corrosion potentials for the anode and cathode are measured to establish corrosion initiation. The corrosion current and the rate of corrosion are determined by measuring the voltage drop across the resistor.

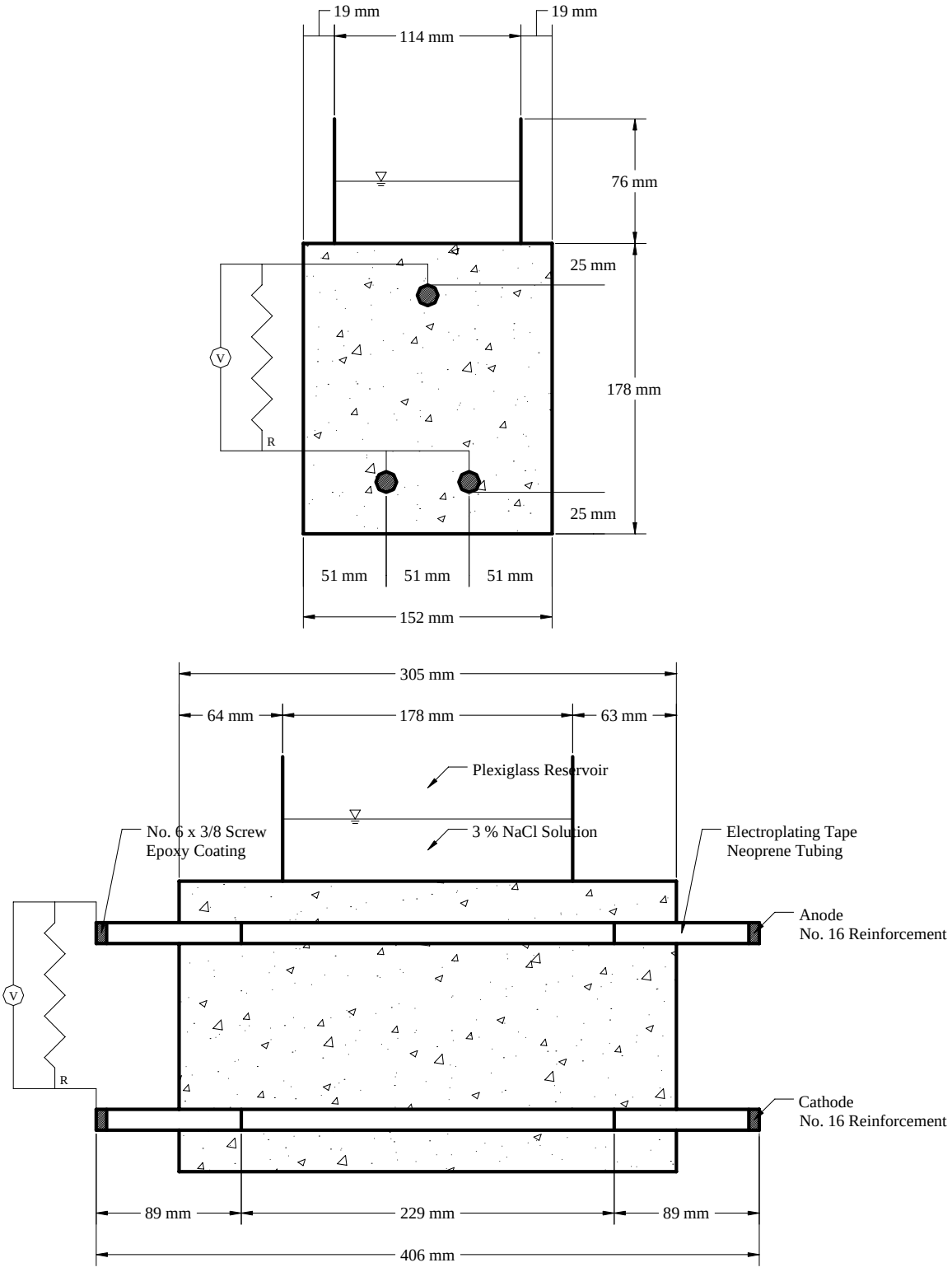

(a) Schematic of ASTM G 109 ACT

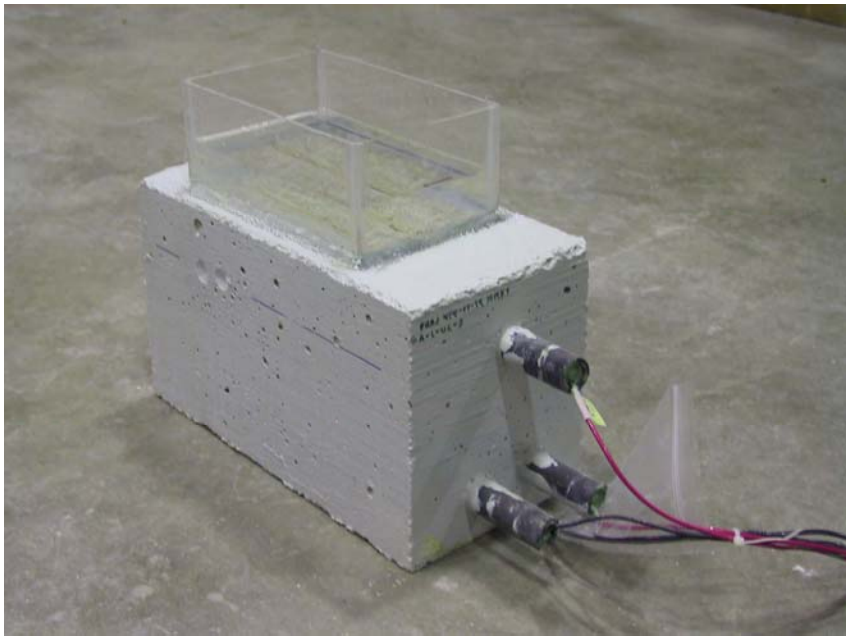

(b) Typical as-constructed ASTM G 109 ACT

Figure 5.1. Accelerated corrosion test specimen

5.2.1.3. Accelerated Corrosion Test Monitoring

Half-cell potentials are measured using a reference electrode. To avoid interference from the other steel elements, the steel reinforcement layers are isolated (i.e., each bar is disconnected from the resistor) before measuring half-cell potential. After the measurements are taken, the steel elements are again electrically connected through the resistor. The half-cell corrosion potential of the anode and cathode are measured using a saturated calomel electrode. The half-cell is maintained in accordance with ASTM C 876 for the stabilization of corrosion potential. The associated corrosion conditions with varying half-cell corrosion potentials from the saturated calomel electrode are listed in Table 5.3 (Broomfield 1997). In the present study, a corrosion potential more positive than 276 mV was considered to be active corrosion.

5.2.2. Accelerated Corrosion Test Specimens

A total of 22 specimens were tested following the ASTM ACT to study the corrosion behavior when chlorides have rapid access to the reinforcement. Table 3.4 lists the test specimens and associated designations used to refer to all tests specimens in this report.

In both the ASTM ACT and the Rapid Macrocell ACT, the MMFX, epoxy-coated reinforcement, and uncoated reinforcement were tested in the as-delivered condition. Two additional conditions for the epoxy-coated reinforcement were also evaluated. First, the epoxy coating was breeched by four 1/8 in. diameter holes drilled in line equidistantly along the reinforcement length. Also evaluated were epoxy-coated reinforcement specimens for which the coating was chipped off at random locations with a razor blade, removing a total area of approximately 64 mm^2 (2.5 sq. in.) of the original coating.

Table 5.3. ASTM criteria for corrosion of steel in concrete for the saturated calomel reference electrode (Broomfield 1997)

Corrosion potential	Corrosion condition
Less than 126 mV	Low (10% risk of corrosion)
126 mV to 276 mV	Intermediate corrosion risk
Greater than 276 mV	High (90% risk of corrosion)
Greater than 426 mV	Severe corrosion risk

Table 5.4. Accelerated corrosion test program

Specimen identification	NaCl concentration	Number of specimens
A[1]-L[2] mmFX[3]	3%	3
A-T[4] mmFX	3%	2
A-L-UC[5]	3%	3
A-T-UC	3%	2
A-L-EC[6]-AD[7]	3%	3
A-T-EC-AD	3%	2
A-L-EC-DH[8]	3%	3
A-T -EC-DH	3%	2
A-T -EC-CH[9]	3%	2
RM[10] mmFX	3%	6
RM-UC	3%	6
RM-EC-AD	3%	6
RM -EC-DH	3%	6

1 A – ASTM G 109 accelerated corrosion test
2 L – Artificial longitudinal crack
3 MMFX – MMFX Microcomposite steel reinforcement
4 T – Artificial Transverse cracks
5 UC – Uncoated mild steel reinforcement
6 EC – Epoxy-coated mild steel reinforcement
7 AD – As-delivered epoxy coating condition
8 DH – Drilled holiday epoxy coating condition
9 CH – Chipped holiday epoxy coating condition
10 RM – Rapid Macrocell accelerated corrosion test

5.2.2.1. ASTM G 109 Accelerated Corrosion Test Specimen

The 22 ASTM ACT concrete beams were cast in a single set of formwork. As illustrated in Figure 5.1, the beams were cast to be 152 mm (6 in.) in width, 178 mm (7 in.) in height, and 305 mm (12 in.) in length. The forms were constructed with holes in the appropriate locations to position the No. 16 (No. 5) reinforcement to maintain exactly 25 mm (1 in.) of clear cover.

Concrete was placed in two layers and consolidated by internal vibration. A float finish was used after consolidation to finish the top surface of the specimen. Additional non-reinforced concrete beams were cast for background chloride analysis.

To provide a direct path for chlorides to the top layer of steel reinforcement, an artificial crack was fabricated in the specimens. The cracks were oriented either parallel or perpendicular to and directly above the top steel reinforcement through the insertion and removal of a 0.3 mm (0.012 in.) stainless steel shim when the specimen was fabricated. The shim was removed within 24 hours of concrete placement, leaving a direct path for chlorides to the steel reinforcement and simulating the effects of a crack over a bar.

The No. 16 (No.5) reinforcement used in these specimens was cut to a length of 406 mm (16 in.), and both ends were ground to remove any sharp edges. One end of each bar was drilled to a depth of 13 mm (0.5 in.) to accommodate a self-tapping No. 6 x 3/8 stainless steel sheet metal screw. The bars were soaked in hexane until clean of grease, dirt, and hydraulic fluid and were allowed to air dry. Each end of the bar was wrapped with electroplating tape so that only a 229 mm (9 in.) length in the middle of the bar was exposed. A 89 mm (3.5 in.) length of neoprene tubing was then placed over the electroplating tape at each end of the bar. The length of tubing protruding from the bar ends was filled with two applications of 3M Scotchkote 413/215 PC Patch Compound two-part epoxy to prevent the bar ends from corroding due to external interference.

The bars were placed in the forms so that the 229 mm (9 in.) bare region was centered within the concrete. A single bar was placed in the top reinforcement layer, while two bars were placed in the bottom layer. The epoxy-coated mild steel reinforcement with drilled holidays was placed with the line of holes facing the top surface to simulate a worst-case scenario. The epoxy-coated mild steel reinforcement with chipped holidays was randomly breeched, with no particular attention paid to the alignment of these holidays. The two layers of steel reinforcement were connected electrically across a 10 ohm resistor.

Following concrete placement, the beams were covered with wet burlap and plastic sheets for the initial curing process. The specimens were then stripped from the forms and cured under the wet burlap and plastic sheets until they were aged 21 days. The top test surfaces were slightly sanded at 18 to 20 days to remove the portland cement skin or laitance, which normally wears off by natural weathering. At 21 days, the specimens were then stored on their sides in air in a laboratory room at 68°F to 78°F for 7 days. At approximately 28 days, the four sides and bottom of each test specimen were coated with two applications of Sierra Performance Manufacturing two-part epoxy concrete paint to minimize lateral moisture movement in the specimens during the tests.

A Plexiglas reservoir, 114 mm (4.5 in.) in width by 178 mm (7 in.) in length by 76 mm (3 in.) in height, was attached to the specimens, as depicted in Figure 5.1. A silicone caulk was used to seal the reservoir from the outside, and the epoxy sealer was applied to the top surface of the specimen outside of the reservoir.

5.2.2.2. Rapid Macrocell Accelerated Corrosion Test Specimen

As illustrated in Figure 5.2, No. 16 (No. 5) reinforcement was cut to a length of 127 mm (5 in.) for the Rapid Macrocell ACT. One end of the reinforcement was then drilled to a depth of 13 mm (0.5 in.) to accept a self-tapping No. 6 x 3/8 stainless steel sheet metal screw, and both ends

were ground to remove sharp edges. The bars were then soaked in hexane to remove grease, dirt, and hydraulic fluid from the surface and the dried at room temperature. The end of the epoxy-coated reinforcement that was to be submerged was protected using 3M Scotchkote 413/215 PC Patch Compound two-part epoxy.

Three cylindrical mortar-clad bars were necessary for each laboratory test system. A single mortar-clad bar was cast in a 38 mm (1.5 in.) diameter PVC pipe to serve as the system anode. The bar was centered in the mold with the mortar sheathing covering the exterior surface of the bar and projecting 25 mm (1 in.) past one end of the reinforcement. Two mortar-clad bars were cast in a 76 mm (3 in.) diameter PVC pipe to serve as the system cathode. Similarly, these bars were centered in the mold, with the mortar sheathing covering the exterior surface of the bar. However, for the cathode, the mortar sheathing projected 76 mm (3 in.) past one end of the reinforcement. The mix proportions for the mortar were the same as the concrete used in the ASTM ACT specimens. The concrete was placed in the cylindrical mold in two layers. Each layer was rodded 25 times using a 3.2 mm (1/8 in.) diameter rod, followed by external vibration for 30 seconds.

Specimens were cured in the molds for 24 hours and then removed from the molds and cured in saturated water for 13 days. After 14 days of curing, the specimens were dried for one day. For the mortar-clad specimens, a 14-guage copper electrical wire was then secured to the tapped end of each specimen with a self-tapping No. 6 x 3/8 stainless steel sheet metal screw. The top of the screw, exposed wire, and concrete were then coated with two applications of 3M Scotchkote 413/215 PC Patch Compound two-part epoxy and Sierra Performance Manufacturing two-part epoxy concrete paint, respectively.

The Rapid Macrocell ACT salt bridge described previously serves as an ionic pathway between the containers holding the specimens. Each salt bridge is made using a 0.9 m (36 in.) long flexible Tygon tube with an inner diameter of 6.4 mm (1/4 in.) and an outside diameter of 9.5 mm (3/8 in.). The tube is filled with a salt gel made from 4.5 g (0.16 oz.) of agar, 30 g (1.06 oz.) of potassium chloride (KCl), and 100 g (3.52 oz.) of distilled water, a quantity of ingredients adequate to make three salt bridges.

The salt gel is made by thoroughly mixing the agar and potassium chloride powders together. The mixture is then combined with distilled water and placed over a Bunsen burner. While heating over the Bunsen burner, the three constituents (agar, KCl, and distilled water) are stirred to a consistency of syrup. The semisolid gel is poured into the tubing. At this point, the completed salt bridge is heated in a container of boiling water for approximately four hours. The salt bridge is taken out of the boiling water and allowed to cool at room temperature. If the semisolid gel does not fully fill the tube (i.e., voids are present) the salt bridge is discarded.

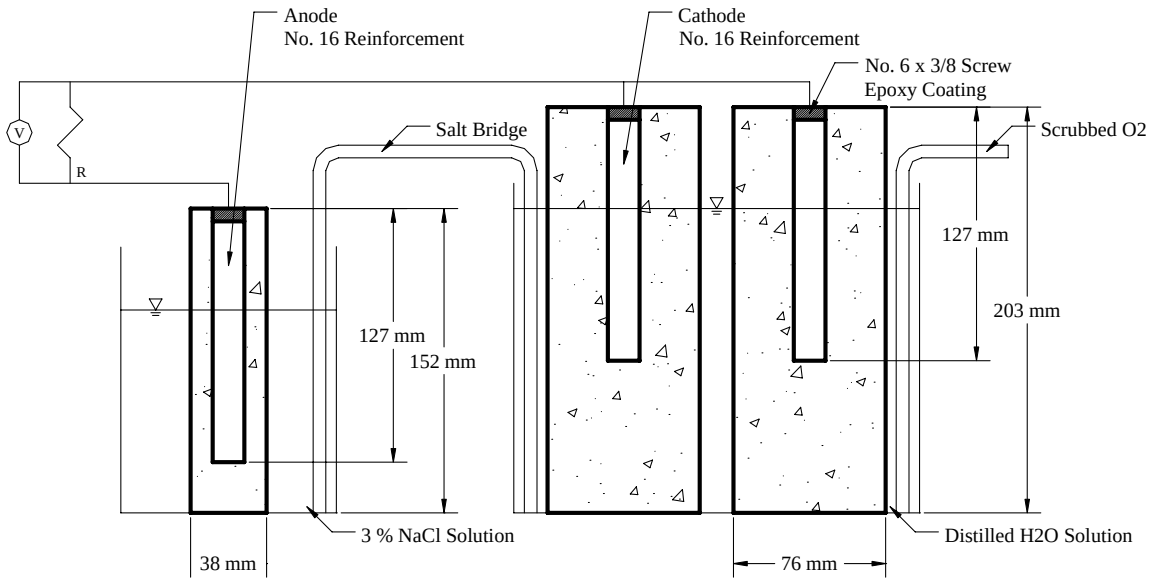

(a) Schematic of Rapid Macrocell ACT

(b) Typical as-constructed Rapid Macrocell ACT

Figure 5.2. Schematic of Rapid Macrocell accelerated corrosion test specimen

5.2.3. Chloride Exposure Protocol

The ASTM ACT chloride exposure condition used in this study was based on a weekly cycle. The beams were subjected to a seven-day ponding and drying regime. For the first four days of each week, the test surface was ponded with a depth of approximately 38 mm (1.5 in.) of 3% sodium chloride solution in the laboratory at 68°F to 78°F. During this period, the reservoir was covered with a plastic sheet to minimize evaporation. Following this four-day exposure, the sodium chloride solution was removed, and the test surface was rinsed with distilled water and drained.

These unponded beams remained dry for three days in the laboratory at 68°F to 78°F. After this exposure, the test surface was immediately reponded with the 3% sodium chloride solution. The ponding and drying regime was continued for 12 weeks, after which the test surface was subjected to continuous ponding for 12 weeks. Following the 12-week period of continuous ponding, the alternating ponding and drying regime was resumed and continued alternatively for the remainder of the test period.

For the Rapid Macrocell ACT, the mortar-clad specimen was placed in a one-quart container, along with a simulated pore solution containing a 3% concentration of sodium chloride for the duration of the test period. When needed, a simulated pore solution was added to maintain the 76.2 mm (3 in.) of reinforcement below the surface.

6. LABORATORY TEST RESULTS

The test results in the following section describe the corrosion resistance performance of MMFX, epoxy-coated mild reinforcement, and uncoated mild steel reinforcement. Specific findings are presented in terms of half-cell voltage (corrosion potential) for the ASTM G 109 ACT and Rapid Macrocell ACT. For reference, the different reinforcement types for each ACT specimen are distinguished by line type in the same figure. The designation for each specimen type is listed in Table 3.4.

6.1. ASTM G 109 Accelerated Corrosion Test

As discussed above, to leave a direct path for chlorides to the top layer of steel reinforcement, an artificial crack, oriented either longitudinally or transversely, was fabricated in the ASTM G 109 specimens. The following sections summarize the test results for each of these crack types.

6.1.1. Results for Longitudinally Cracked Specimens

Figures 6.1 (a) and (b) show the 609-day (87-week) average anode (top reinforcement layer) and cathode (bottom reinforcement layer) corrosion potentials for specimens with a longitudinal artificial crack over the top and bottom layers of steel reinforcement, respectively.

For the MMFX reinforcement with longitudinally cracked specimens, the corrosion potential for the top layer of reinforcement (anode) remained at a relatively constant value of 100 mV through 217 days (31 weeks). At 217 days, a single MMFX specimen began corroding, which caused the rapid and continued increase to 437 mV by 609 days (87 weeks).

The corrosion potential for all the uncoated reinforcement specimens increased beyond 276 mV (i.e., high risk of corrosion) by 35 days (5 weeks). After 35 days, the uncoated specimens had a corrosion potential greater than 400 mV. The corrosion potential rose to a maximum of 493 mV at 245 days (35 weeks) and remained constant through 609 days (87 weeks). This indicates a continued severe risk for corrosion.

Specimens with the as-delivered epoxy-coated reinforcement exhibited a relatively constant corrosion potential of around 25 mV through 609 days (87 weeks), indicating a low risk for corrosion.

The corrosion potential for the drilled holiday epoxy-coated reinforcement experienced spikes of 300 mV throughout days 105 to 217 (weeks 15 to 31), as the specimens began to corrode throughout the interval. The corrosion potential rose to a maximum of 430 mV at 224 days (32 weeks), but decreased to 219 mV through 609 days (87 weeks), indicating that the corrosion had ceased.

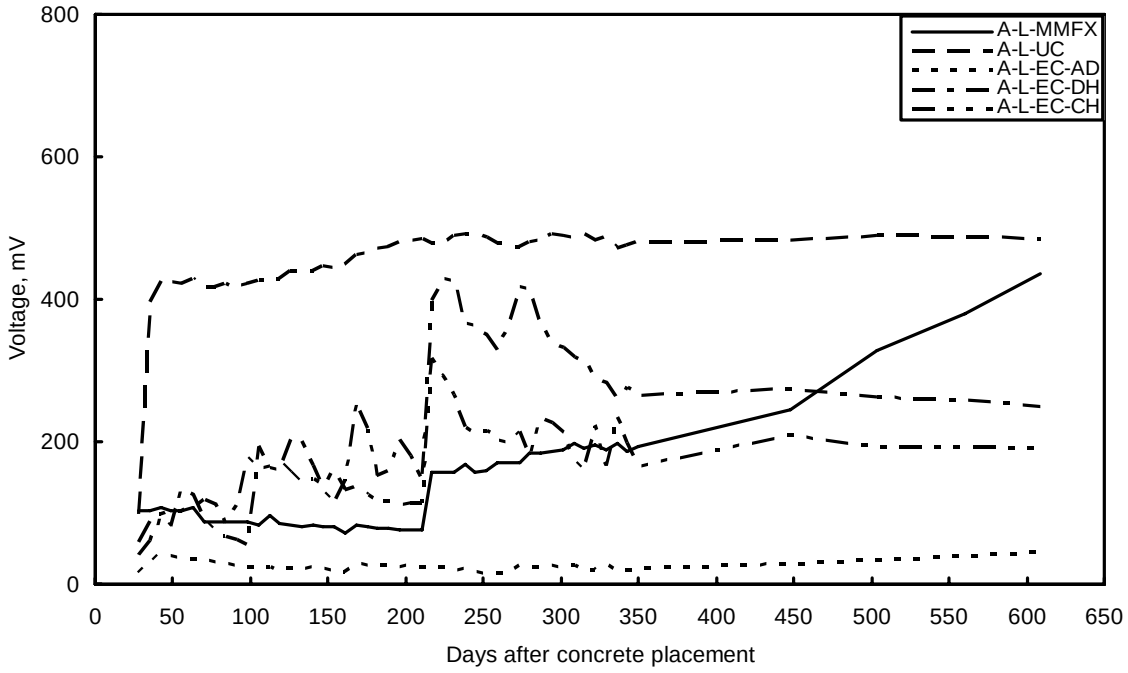

(a) Corrosion risk of the top layer of steel reinforcement

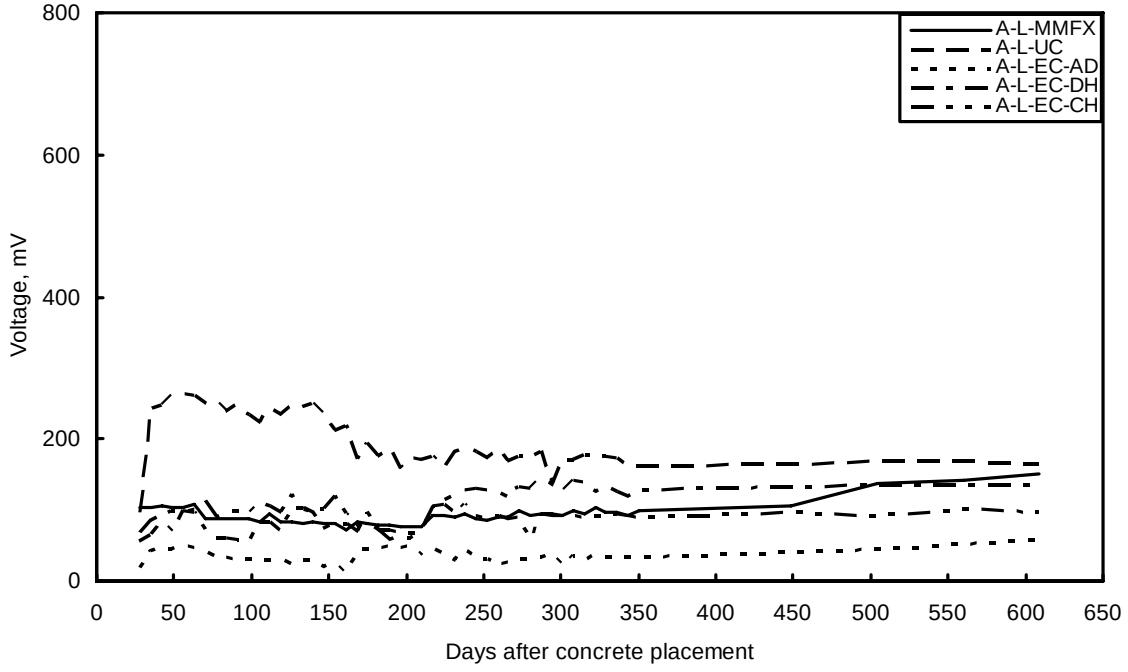

(b) Corrosion risk of the bottom layer of steel reinforcement

Figure 6.1. ASTM G 109 ACT subjected to 3% NaCl solution through longitudinal crack

The chipped holiday condition of the epoxy-coated reinforcement exhibited a corrosion potential of 100 mV through the first 217 days (31 weeks). At 217 days, a single specimen began corroding, which caused the maximum average corrosion potential of 316 mV. However, by 350 days (50 weeks), the corrosion potential value decreased and remained constant at approximately 200 mV.

The corrosion potential for the bottom layer of reinforcement (cathode) for all reinforcement types remained below 276 mV, indicating that none had undergone active corrosion (see Figure 6.1 [b]). Additionally, no corrosion products were observed on the concrete surfaces of any of the test specimens.

6.1.2. Results for Transversely Cracked Specimens

Figures 6.2 (a) and (b) show the 609-day (87-week) average anode (top reinforcement layer) and cathode (bottom reinforcement layer) corrosion potentials for specimens with transverse artificial cracks over the top and bottom layers of steel reinforcement, respectively.

For the MMFX reinforcement with transversely cracked specimens, the corrosion potential for the top layer of reinforcement (anode) remained at a relatively constant value of 80 mV through 280 days (40 weeks), indicating a low risk for corrosion. At 350 days, however, a single MMFX specimen began corroding, which caused a rapid increase to 257 mV at 609 days (87 weeks).

Similar to the corrosion potentials for the longitudinally cracked specimens, the corrosion potentials for all the uncoated reinforcement specimens with transverse cracks increased beyond 276 mV by 35 days (5 weeks). By 98 days (14 weeks), the uncoated specimens experienced a corrosion potential value greater than 400 mV, which continued to rise to 530 mV through 609 days (87 weeks), indicating a continued severe risk for corrosion.

Specimens with as-delivered epoxy-coated reinforcement exhibited relatively constant corrosion potential values of 20 mV through 161 days (23 weeks). At 161 days, a single specimen began corroding, causing a rapid increase in the average corrosion potential and the constant corrosion potential, which was 300 mV through 322 days (46 weeks). The corrosion potentials decreased to 235 mV through 609 days (87 weeks).

Similar to the longitudinally cracked specimens, the drilled holiday epoxy-coated reinforcement with transverse cracks experienced spikes of 250 mV throughout days 105 to 217 (weeks 15 to 31) as the specimens began to corrode. However, due to continued decrease in corrosion potential, the 609-day (87-week) corrosion potential was 144 mV.

The corrosion potential for the bottom layer of reinforcement (cathode) for all reinforcement types remained below 276 mV, indicating that none had undergone active corrosion. Additionally, no corrosion products were observed on the concrete surface for any of the test specimens.

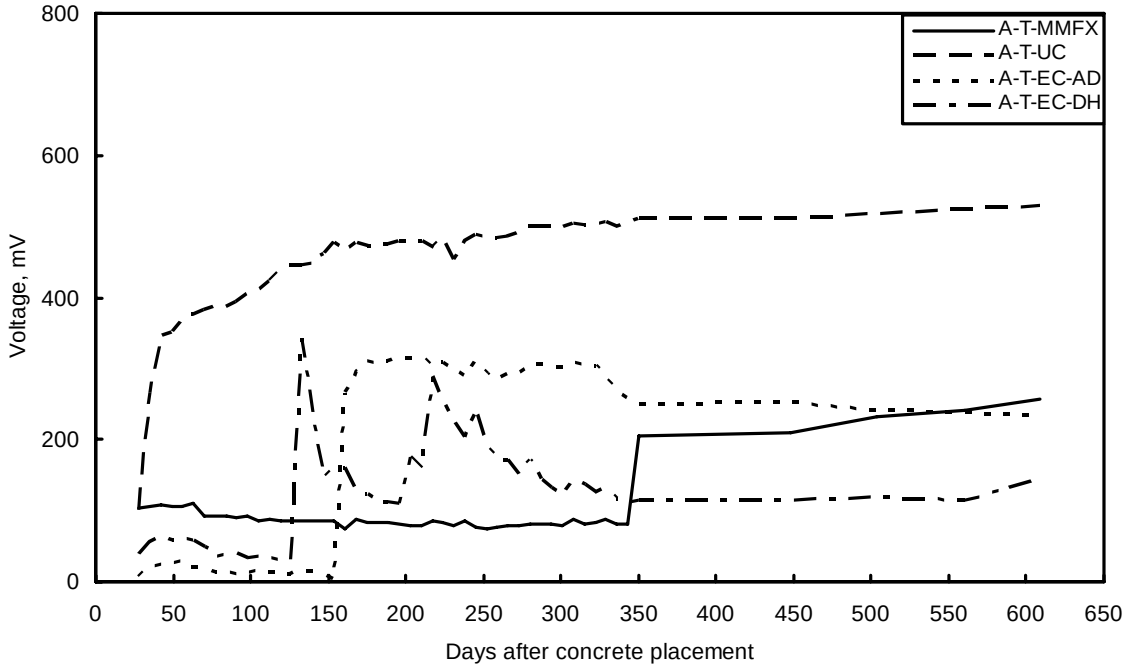

(a) Corrosion risk of the top layer of steel reinforcement

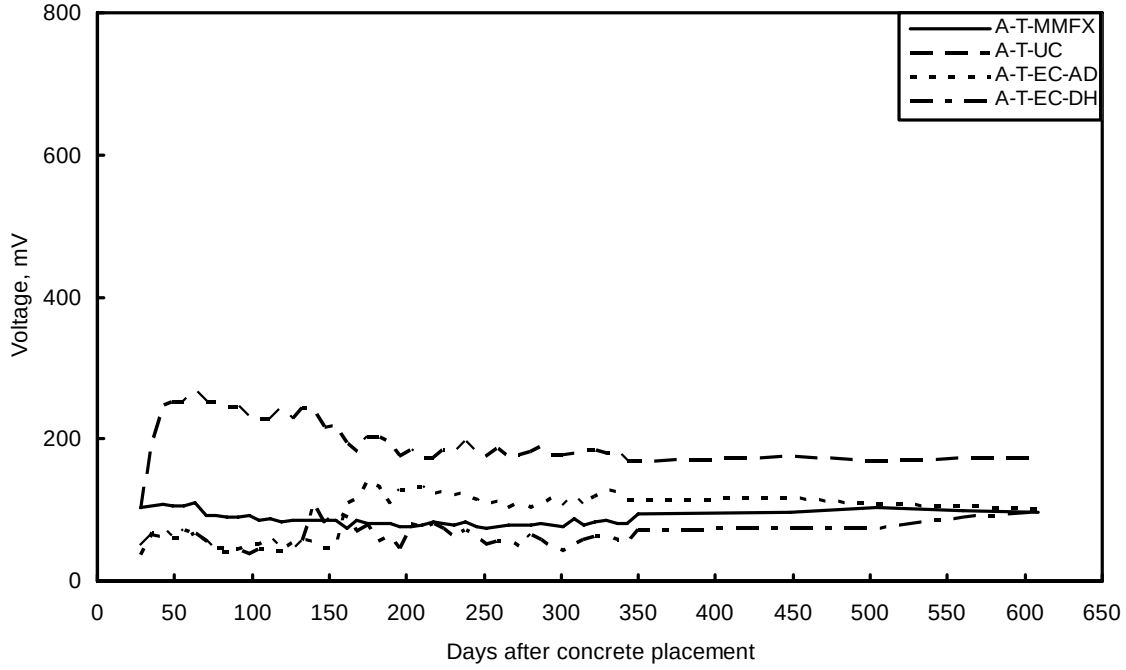

(b) Corrosion risk of the bottom layer of steel reinforcement

Figure 6.2. ASTM G 109 ACT subjected to 3% NaCl solution through transverse crack

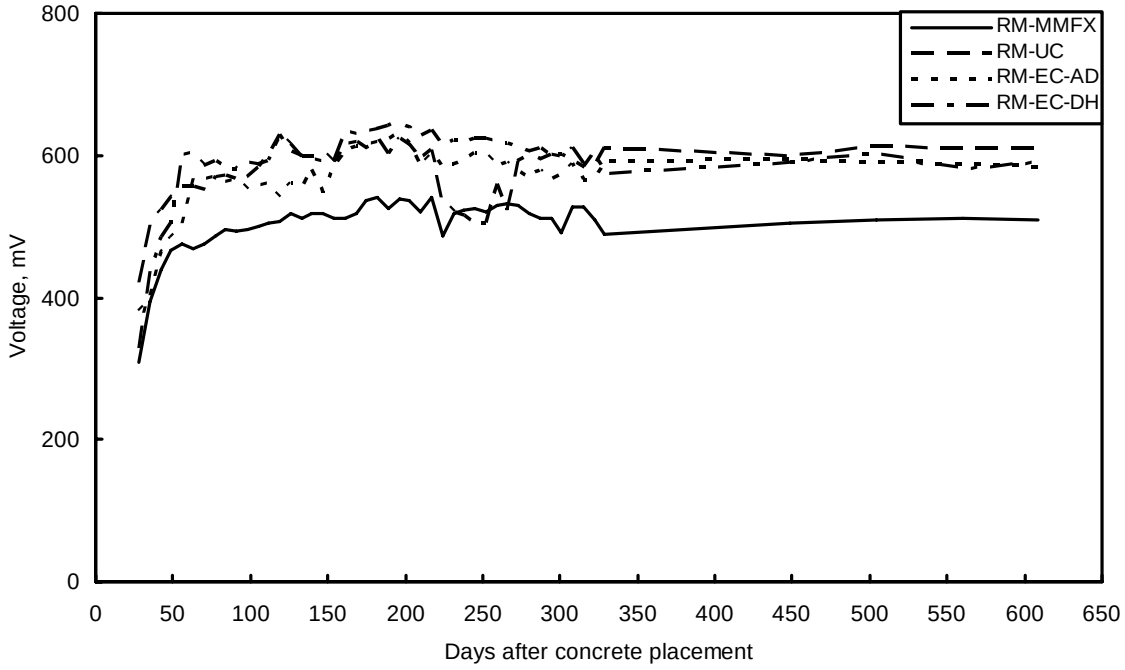

(a) Corrosion risk of the top layer of steel reinforcement

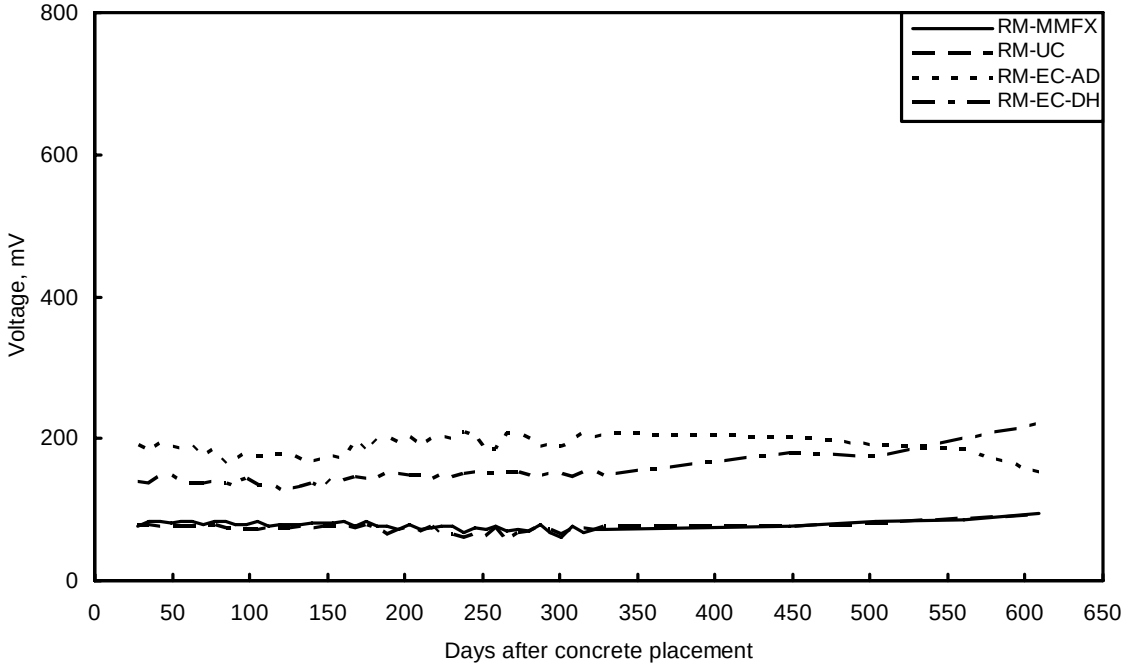

(b) Corrosion risk of the bottom layer of steel reinforcement

Figure 6.3. Rapid Macrocell ACT subjected to 3% NaCl solution

6.2. Rapid Macrocell Accelerated Corrosion Test

Figure 6.3 shows the 609-day (87-week) average corrosion potentials for the anode steel reinforcement (reinforcement in the container with sodium chloride solution) and cathode steel reinforcement (reinforcement in the container with distilled water).

Within 35 days (5 weeks), all reinforcement types in the container with 3% sodium chloride solution (anode) were undergoing corrosion. Through 609 days (87 weeks), the MMFX reinforcement experienced a constant corrosion potential of 500 mV.

From 105 to 217 days (15 to 31 weeks), the uncoated reinforcement specimens exhibited a corrosion potential of 600 mV. At 217 days and continuing through 273 days (39 weeks), a single specimen ceased corroding, which caused the average corrosion potential to decrease to 515 mV. After 273 days, the corrosion potential returned to 600 mV.

After 280 days (40 weeks), the as-delivered epoxy-coated specimens experienced a constant corrosion potential of 600 mV. Similar to the as-delivered epoxy-coated specimens, the drilled holiday epoxy-coated specimens experienced a constant corrosion potential of 600 mV.

The corrosion potential for all reinforcement types in the container with distilled water (cathode) remained below 276 mV, indicating that none had undergone active corrosion. With the exception of the as-delivered and drilled holiday conditions of epoxy-coated reinforcement, corrosion products were visually observed on the mortar sheathing and within the solution of the anode.

After the completion of corrosion monitoring in the laboratory, the specimens were carefully broken and the reinforcing bars were collected. These bars were visually examined for corrosion and section losses. Figures 6.4 and 6.5 show selected reinforcing bars collected at the end of the test period. This aspect of the study revealed that some discoloration was associated with the different type of reinforcing steel used in the test specimens. In addition, the results indicated that the corrosion associated with the uncoated bars was more significant than that associated with the MMFX bars. No corrosion or section losses were observed for the epoxy-coated bars.

6.3. Chloride Ion Concentration

To investigate the chloride ion concentration in the ASTM ACT specimens, concrete powder samples were collected once corrosion initiation was identified. Recall that two unreinforced beams were cast at the same time as the other laboratory ACT specimens for supplementary chloride analysis. Powder samples were collected as soon as corrosion initiated and were collected at intervals of 90 days to monitor the ingress of chlorides. This process was carried out for the first 270 days of the laboratory testing program.

Figure 6.4. Corded uncoated reinforcing bar

Figure 6.5. Corded MMFX reinforcing bar

6.3.1. Cement Mortar Powder Collection

When the various electrochemical investigations indicated corrosion initiation (i.e., 276 mV) for the individual ASTM ACT specimens, concrete powder samples were collected at the depth of the top reinforcement (anode) layer using a hammer drill with a stop gage, as described by ASTM C 1152/C 1152 M (Standard Test Method for Acid-Soluble Chloride) and ASTM C 1218/C 1218 M (Water-Soluble Chloride in Mortar and Concrete) (ASTM 2001a; ASTM 2001b). The procedure was as follows:

1. The specimen was marked for two adjoining holes to be drilled to obtain a representative sample of at least 20 grams (0.71 oz.) of concrete powder.
2. A drill bit was selected to ensure that the majority of the powder collected was cement mortar and not coarse aggregate (15.88 mm [5/8 in.], 1.5 times larger than the nominal course aggregate). Each of the adjoining holes was first drilled to a depth of 12.7 mm (1/2 in.). After drilling both initial holes, the powder was vacuumed from each hole and discarded and the top surface blown clean. The final 15.88 mm (5/8 in.) diameter holes were then drilled. No lubricants were used during drilling.
3. The powder from the two adjoining holes was removed and combined into the first composite sample in a bag, and the specimen ID was recorded on the bag.
4. To prevent sample contamination, contact between the sample material and hands or other sources of perspiration was avoided. All other sampling tools were cleaned and dried prior to each sampling operation.
5. The process was repeated for each specimen to obtain a second composite powder sample, for a total of two composite samples for each ASTM ACT specimen.

From the two composite samples described for each ASTM ACT specimen, an average specimen chloride ion concentration was determined.

6.3.2. Chloride Ion Concentration

The collected powder samples were tested using the Phillips PW 2404 X-ray fluorescence (XRF) spectrometer at the Iowa State University Material Analysis and Research Laboratory. XRF spectroscopy provides a means to identify and quantify the concentration of elements contained in a solid, powdered, and liquid sample.

6.3.3. Chloride Ion Concentration Results

The chloride ion content data collected from the powder samples were used to determine a comparative chloride ion concentration for each reinforcement type after the first high corrosion risk was measured (i.e., 276 mV). The average results are shown in Table 6.1. Additionally, the chloride ion concentrations of the concrete were also analyzed at 90-day intervals to verify that the rate of chloride ingress was similar among all ASTM ACT specimens.

6.3.3.1. MMFX Microcomposite Steel Reinforcement

Only one specimen containing MMFX reinforcement provided measurements that indicated high corrosion risk (i.e., 276 mV). Subsequently, powder samples from that specimen were collected, and the chloride ion concentration was measured in terms of weight concentration per cubic yard. This MMFX reinforcement specimen had a chloride ion concentration of 1.62 kg/m^3 (2.73 lb./cu. yd.). This value is lower than the chloride ion concentrations of 1.97 and 2.14 kg/m^3 (3.32 and 3.60 lb./cu. yd.) published by the University of Kansas Center for Research.

6.3.3.2. Uncoated Mild Steel Reinforcement

High corrosion risk had been measured for all five specimens containing uncoated reinforcement. The corresponding chloride ion concentration values ranged from a low of 0.61 kg/m^3 (1.03 l lb./cu. yd.) to a high of 0.66 kg/m^3 (1.11 lb./cu. yd.), with an average value of 0.63 kg/m^3 (1.06 lb./cu. yd.). These values match those obtained in earlier studies.

6.3.3.3. As-Delivered Epoxy-Coated Mild Steel Reinforcement

As shown in Table 6.1, the laboratory test data indicate that one specimen containing the as-delivered epoxy-coated reinforcing bar exhibited some corrosion after 133 days. The chloride ion concentration in the concrete surrounding the reinforcing bars was determined to be approximately 1.16 kg/m^3 (1.96 lb./cu. yd.). No other specimen indicated that corrosion had initiated, though the measured chloride ion concentration was higher than 1.16 kg/m^3 (1.96 lb./cu. yd.) (see Table 6.1). For example, Table 6.1 shows that no corrosion seemed to have initiated in specimen A-T-EC-AD(2), though the chloride ion concentration reached 1.77 kg/m^3 (2.99 lb./cu. yd.). Therefore, one may conclude that a chloride ion concentration greater than 1.77 kg/m^3 (2.99 lb./cu. yd.) would be needed to initiate corrosion of epoxy-coated reinforcing bars in as-delivered conditions. However, strict examination of the as-delivered epoxy-coated bars at the construction site of a bridge structure should determine whether the coating layer is damaged. This damage may accelerate the initiation of corrosion in epoxy-coated bras (see Section 6.3.3.4).

6.3.3.4. Drilled Holiday Epoxy-Coated Mild Steel Reinforcement

All five epoxy-coated reinforcement specimens containing the drilled holidays experienced high corrosion risk measurements (see Table 6.1). Chloride ion concentration values for these specimens ranged from a low of 0.68 kg/m^3 (1.14 lb./cu. yd.) to a high of 1.67 kg/m^3 (2.82 lb./cu. yd.) with an average value of 1.03 kg/m^3 (1.74 lb./cu. yd.).

6.3.3.5. Chipped Holiday Epoxy-Coated Mild Steel Reinforcement

High corrosion risk was measured for a single epoxy-coated reinforcement specimen with the chipped holiday condition. The corresponding chloride ion concentration value was 1.23 kg/m^3 (2.08 lb./cu. yd.).

Table 6.1. Chloride-ion concentration at corrosion initiation and 90-day intervals

Specimen identification	Chloride ion at corrosion initiation		90-day chloride ion concentration	180-day chloride ion concentration	270-day chloride ion concentration
	Time, days	Concentration, kg/m^3 (pcy)	Concentration, kg/m^3 (pcy)	Concentration, kg/m^3 (pcy)	Concentration, kg/m^3 (pcy)
A-L mmFX (1)	189	1.62 (2.73)	0.95 (1.60)	1.52 (2.56)	1.76 (2.96)
A-L mmFX (2)			0.80 (1.34)	1.16 (1.95)	1.41 (2.38)
A-L mmFX (3)					0.78 (1.32)
A-T mmFX (1)					1.02 (1.72)
A-T mmFX (2)					1.51 (2.54)
MMFX Average		*1.62 (2.73)*	*0.87 (1.47)*	*1.33 (2.25)*	*1.29 (2.18)*
A-L-UC (1)	7	0.62 (1.05)	0.80 (1.34)	1.03 (1.74)	1.10 (1.85)
A-L-UC (2)	7	0.66 (1.11)	0.80 (1.35)	1.25 (2.10)	1.98 (3.34)
A-L-UC (3)	7	0.61 (1.03)			1.19 (2.00)
A-T-UC (1)	7	0.63 (1.07)			1.27 (2.14)
A-T-UC (2)	14	0.61 (1.03)			1.50 (2.52)
UC Average		*0.63 (1.06)*	*0.80 (1.34)*	*1.14 (1.92)*	*1.41 (2.37)*
A-L-EC-AD (1)			0.80 (1.35)	1.09 (1.83)	1.15 (1.93)
A-L-EC-AD (2)			0.87 (1.47)	1.15 (1.93)	1.71 (2.88)
A-L-EC-AD (3)					1.32 (2.23)
A-T-EC-AD (1)	133	1.16 (1.96)			1.44 (2.42)
A-T-EC-AD (2)					1.77 (2.99)
EC-AD Average		*1.16 (1.96)*	*0.84 (1.41)*	*1.12 (1.88)*	*1.48 (2.49)*
A-L-EC-DH (1)	77	0.68 (1.14)	0.69 (1.16)	0.94 (1.58)	1.30 (2.19)
A-L-EC-DH (2)	77	0.71 (1.20)	0.71 (1.20)	1.03 (1.74)	1.60 (2.69)
A-L-EC-DH (3)	98	0.85 (1.43)			2.18 (3.68)
A-T-EC-DH (1)	189	1.25 (2.10)			1.55 (2.61)
A-T-EC-DH (2)	105	1.67 (2.82)			1.97 (3.32)
EC-DH Average		*1.03 (1.74)*	*0.70 (1.18)*	*0.98 (1.66)*	*1.72 (2.90)*
A-L-EC-CH (1)					1.19 (2.00)
A-L-EC-CH (2)	189	1.23 (2.08)			1.55 (2.61)
EC-CH Average		*1.23 (2.08)*			*1.37 (2.31)*

6.4. Discussion of Laboratory Test Results

The results from the mechanical properties tests demonstrate that MMFX microcomposite steel reinforcement has considerably higher yield and tensile strengths but lower elongations than mild steel reinforcement. The lower elongations obtained with MMFX steel are expected for high-strength steels.

The following discussion of the results from the accelerated corrosion tests and chloride ion concentration analyses provides a basis for making corrosion resistance comparisons. While these results are used to make preliminary comparisons, the reader should be aware that a degree

of uncertainty exists. This is especially the case for the MMFX and as-delivered epoxy-coated reinforcement, for which corrosion had initiated in only a single specimen of each type.

At a given time during the testing, significant variation in corrosion potential was observed for specimens containing the same reinforcement type. This variation may have been caused by dissimilarities in anode and cathode locations, epoxy coating performance, and reinforcement material variations. The rates of consumption and renewal of the fundamental factors for sustaining active corrosion (i.e., chloride ions, oxygen, and water) may have also caused specimens reinforced with the same steel type to behave differently (Pfeifer and Scali 1981). However, a reasonable correlation existed when the average of the corrosion potentials for each reinforcement type was compared under the same test conditions.

Through 280 days (40 weeks), the ASTM ACT generally showed evidence of low to intermediate corrosion risk potentials for the MMFX reinforcement, with the exception of a single longitudinally cracked specimen. This specimen began corroding at 217 days (31 weeks). The corrosion potential increased rapidly for the uncoated reinforcement, and after 35 days (5 weeks) all specimens indicated that corrosion had initiated. Longitudinally and transversely cracked specimens with the as-delivered epoxy-coated reinforcement exhibited the lowest corrosion potential, although a single transversely cracked specimen began corroding at 161 days (23 weeks). The corrosion potential for epoxy-coated reinforcement with induced holidays indicated that corrosion initiated in the specimens between 105 to 217 days (15 to 31 weeks). Through 280 days (40 weeks), none of the ASTM ACT specimens showed any visual indication (i.e., deposition of corrosion products or concrete discoloration) of the corrosion of the top reinforcement (anode).

Within the first week, the Rapid Macrocell ACT produced severe corrosion risk potentials for all the reinforcement types. The specimens with MMFX reinforcement had the least severe corrosion risk potential, while the uncoated, as-delivered reinforcement and the epoxy-coated reinforcement with drilled holidays had the most severe corrosion risk potentials. Since the Rapid Macrocell ACT specimens are an alteration of the ASTM ACT beam specimens, the almost immediate severe corrosion risk potentials measured for all the reinforcement types was unexpected. To justify the differing responses between the ASTM and Rapid Macrocell corrosion potentials, the authors suggest the continuous renewal of oxygen in the Rapid Macrocell ACT. By continuously replenishing oxygen, the Rapid Macrocell ACT created an environment more conducive to initiating and sustaining corrosion than the ASTM ACT, which replenished oxygen through the previously described ponding and drying regime. Additionally, the Rapid Macrocell ACT was carried out with a plastic sheet placed over the entire test system. This maintained a high-humidity environment over the portion of the cylindrical test specimen not submerged in the solution.

For the study presented herein, a corrosion potential greater than 276 mV was understood to be indicate corrosion initiation. At the time of the first measurement greater than 276 mV, concrete powder specimens were collected at the top reinforcement depth. The chloride ion concentration for the single specimen containing MMFX reinforcement was 1.62 kg/m^3 (2.73 lb./cu. yd.). This value is lower than the chloride ion concentrations of 1.97 and 2.14 kg/m^3 (3.32 and 3.60 lb./cu. yd.) published by the University of Kansas Center for Research. For uncoated mild reinforcement, the chloride ion concentration obtained was 0.63 kg/m^3 (1.06 lb./cu. yd.). This value matched the values of 0.59 to 0.83 kg/m^3 (1.00 to 1.40 lb./cu. yd.) commonly believed to

be the chloride threshold of uncoated mild steel. For the single specimen containing as-delivered epoxy-coated reinforcement, the chloride ion concentration was 1.16 kg/m^3 (1.96 lb./cu. yd.), while the chloride ion concentration for the epoxy-coated reinforcement with induced holidays was 1.03 kg/m^3 (1.74 lb./cu. yd.). As discussed above, the authors believe the value of 1.16 kg/m^3 (1.96 lb./cu. yd.) may not necessarily represent epoxy-coated reinforcement in a pure as-delivered condition.

7. SUMMARY, CONCLUSIONS, AND RECOMMENDATIONS

7.1. Summary

The corrosion of steel reinforcement in an aging highway infrastructure is a major problem currently facing the transportation engineering community. In the United States, maintenance and replacement costs of deficient bridges are measured in billions of dollars. As a specific example, the use of deicing salts has resulted in the steady deterioration of bridge decks due to corrosion.

These concerns have initiated the continual development of protective measures for RC structures. Corrosion-resistant steel reinforcement, as an alternative reinforcement for existing mild steel reinforced concrete bridge decks, has potential due to the inherent corrosion-resistant properties associated with the material.

To investigate corrosion prevention through the use of corrosion-resistant alloys, MMFX microcomposite steel reinforcement, a high-strength, high-chromium steel reinforcement, was evaluated for corrosion resistance performance. The steel was compared to epoxy-coated and uncoated mild steel reinforcement though separate field and laboratory evaluations. However, because definitive field evidence of the corrosion resistance of MMFX reinforcement may require several years of monitoring, attention was transferred to investigating MMFX reinforcement under accelerated conditions in the laboratory. In the laboratory investigation, the principal emphasis was placed on the corrosion performance of MMFX, epoxy-coated reinforcement, and uncoated reinforcement in standardized tests. The evaluation process was based on the commonly applied ASTM and Rapid Macrocell accelerated corrosion tests.

7.2. Conclusions

The MMFX microcomposite reinforcement exhibited yield strengths approximately twice those required for Grade 60 mild reinforcement. The results from the mechanical properties testing demonstrated that MMFX microcomposite steel reinforcement has considerably higher yield and tensile strengths, but lower elongations than mild steel reinforcement. The lower elongations obtained with MMFX steel were as expected for high-strength steels. The tensile and yield strengths of MMFX steel were closer to those specified for high-strength steel reinforcement for prestressing concrete (ASTM A 722) than they were to mild steel reinforcement (ASTM A 615). For the No. 16 reinforcement, however, while the tensile strengths exceeded the minimum 150 ksi required for A722 reinforcement, the yield strengths, based on 0.2% offset, did not meet the requirements for either Type I or Type II, which were 85% (878.5 MPa or 127.5 ksi) and 80% (826.8 MPa or 120 ksi), respectively, of the minimum tensile strength.

The test results for the present study demonstrate that MMFX microcomposite steel reinforcement is more corrosion-resistant than uncoated mild steel reinforcement and exhibits similar corrosion resistance to epoxy-coated reinforcement that meets the requirements of ASTM A 775. Compared to uncoated reinforcement, MMFX reinforcement requires a higher chloride ion concentration for corrosion initiation. In the field portion of the study, the measurements indicate that corrosion-related measurements were lower for the MMFX bridge than for the

epoxy bridge. However, no significant corrosion activity had been observed in either bridge deck. Through continued monitoring and evaluation, the ongoing field monitoring system is expected to provide evidence of the corrosion resistance of the reinforcements monitored.

After 40 weeks of laboratory testing, the ASTM ACT corrosion potentials indicated that corrosion had not initiated for either MMFX or the as-delivered epoxy-coated reinforcement. However, the uncoated mild steel underwent corrosion within the fifth week, while the epoxy-coated reinforcement with holidays underwent corrosion between 15 and 30 weeks. Within the fifth week of testing, the Rapid Macrocell ACT produced corrosion risk potentials indicative of active corrosion for all reinforcement types tested. All ASTM ACT specimens had essentially identical surface appearances at 12 weeks. However, in the Rapid Macrocell ACT, the concrete surrounding the MMFX and uncoated reinforcement discolored due to deposition of corrosion products.

For the study presented herein, concrete powder specimens were collected at the top reinforcement depth at the first indication of corrosion initiation. For the uncoated mild reinforcement, a chloride ion concentration of 0.63 kg/m^3 (1.06 lb./cu. yd.) at corrosion initiation was obtained. This value matches the value of 0.59 to 0.83 kg/m^3 (1.00 to 1.40 lb./cu. yd.) commonly believed to be the chloride threshold of uncoated mild steel. For the epoxy-coated reinforcement with induced holidays, the chloride ion concentration was 1.03 kg/m^3 (1.74 lb./cu. yd.).

7.3. Recommendations

The following are recommended for future research:

- For the ASTM ACT, only a single specimen reinforced with MMFX microcomposite steel underwent corrosion through 40 weeks of testing. Similarly, only one as-delivered epoxy-coated specimen underwent corrosion. Additional testing should be completed to collect additional data.
- As would be expected after only a year and a half of field monitoring, no measurements indicate corrosion initiation on either field bridge deck being monitored. Continued monitoring of the field bridges will provide more accurate results, reflecting real behavior in the environmental conditions of a bridge constructed in the state of Iowa.
- Through further utilization of the field bridge deck data, further calibration of the life expectancy procedure can be made to predict the time to corrosion initiation and the time between initiation and spalling more accurately.

8. REFERENCES

Abu-Hawash, A. 2005. Iowa Department of Transportation. Personal communication.

ASTM G 109-99a. 2001. Standard Test Method for Determining the Effects of Chemical Admixtures on the Corrosion of Embedded Steel Reinforcement in Concrete Exposed to Chloride Environments. *Annual Book of ASTM Standards*. Vol. 3.02. West Conshohocken, PA: American Society for Testing and Materials. 482–486.

ASTM C 1152/C 1152 M. 2001. Standard Test Method for Acid-Soluble Chloride in Mortar and Concrete. *Annual Book of ASTM Standards*. Vol. 4.02. West Conshohocken, PA: American Society for Testing and Materials. 627–629.

ASTM C 1218/C 1218 M. 2001. Standard Test Method for Water-Soluble Chloride in Mortar and Concrete. *Annual Book of ASTM Standards*. Vol. 4.02. West Conshohocken, PA: American Society for Testing and Materials. 645–647.

Broomfield, J. P. 1997. *Corrosion of Steel in Concrete: Understanding, Investigation, and Repair*. London: Spon Press Publications.

Brown, R. D. 1980. *Mechanisms of Corrosion of Steel in Concrete in Relation to Design, Inspection, and Repair of Offshore and Costal Structures*. Special Publication 65-11. Detroit, MI: American Concrete Institute. 169–204.

Cady, P. D. and E.J. Gannon. 1992. State of the Art Mixing Methods. *Condition Evaluation of Concrete Bridges Relative to Reinforcement in Concrete*. Vol. 1. SHRP-S/FR-92-103. Washington, D.C.: Strategic Highway Research Program, National Research Council.

Chappelow, C. C., A.D. McElroy, R.R. Blackburn, D. Darwin, F.G. deNoyelles, and C.E. Locke. 1992. *Handbook of Test Methods for Evaluating Chemical Deicers*. Washington, D.C.: Strategic Highway Research Program, National Research Council.

Clear, K. C. 1975. *Reinforcing Bar Corrosion in Concrete: Effect of Special Treatments*. Special Publication 49. Detroit, MI: American Concrete Institute. 77–82.

Clear, K. C. 1976. *Time-to-Corrosion of Reinforcing Steel in Concrete Slabs*. FHWA-RD-76-70. Washington, D.C.: Federal Highway Administration.

Darwin, D., J. Browning, T.V. Nguyen, and C.E. Locke. 2002. *Mechanical and Corrosion Properties of a High-Strength, High Chromium Reinforcing Steel for Concrete*. SD2001-05-F. Lawrence, KS: University of Kansas Center for Research.

Fanous, F., H. Wu, and J. Pape. 2000. *Impact of Deck Cracking on Durability*. CTRE Management Project 97-5. Ames, IA: Center for Transportation Research and Education.

Fliz, J., S. Akshey, D. Li, Y. Kyo, S. Sabol, H. Pickering, and K. Osseo-Asare. 1992. Method for Measuring the Corrosion Rate of Steel in Concrete. *Condition Evaluation of Concrete Bridges Relative to Reinforcement Corrosion*. Vol. 2. Washington, D.C.: Strategic Highway Research Program, National Research Council.

Gaal, G. C., C. van der Veen, and M.H. Djorai. 2001. Chloride Threshold: State of the Art. The Netherlands.

Hausmann, D. A. 1967. Steel Corrosion in Concrete: How Does it Occur? *Materials Protection* 6.19. 19–23.

Herald, S. E. 1989. The Development of a Field Procedure for Determining the Chloride Content of Concrete and an Analysis on the Variability of the Effective Diffusion Constant. Master's Thesis, Virginia Polytechnic and State University.

Lee, Y. S. 2003. Evaluation of Bridges Strengthened or Newly Constructed with Innovative Materials. Master's Thesis, Iowa State University.

Locke, C. E. 1986. Corrosion of Steel in Portland Cement Concrete: Fundamental Studies. *Corrosion Effects of Stray Currents and the Techniques for Evaluating Corrosion of Rebars in Concrete*. ASTM STP 906. Philadelphia, PA: American Society for Testing and Materials. 5–14.

Manning, D. G. 1996. Corrosion Performance of Epoxy-Coated Reinforcing Steel: North American Experience. *Construction and Building Materials* 10.5. 349–365.

Martinez, S. L., D. Darwin, S.L. McCabe, and C.E. Locke. 1990. *Rapid Test for Corrosion Effects of Deicing Chemicals in Reinforced Concrete*. SL Report 90-4. Lawrence, KS: University of Kansas Center for Research.

MMFX Technologies Corporation. 2005. *Setting the Standards for the Future*. http://www.mmfxsteel.com/.

Pape, J. J. 1998. Impact of Bridge Deck Cracking on Durability. Master's Thesis, Iowa State University.

Pfeifer, D. W. 2000. High Performance Concrete and Reinforcing Steel with a 100-Year Service Life. *PCI Journal* 45.3. 46–54.

Pfeifer, D. W. and M.J. Scali. 1981. *Concrete Sealers for Protection of Bridge Structures*. NCHRP Report 244. Washington, D.C.: Transportation Research Board.

Sagues, A. A., R.G. Powers, and C.E. Locke. 1994. *Corrosion Processes and Field Performance of Epoxy-Coated Reinforcing Steel in Marine Structures*. Corrosion 94. Paper No. 299. Houston, TX: NACE International.

Sagues, A. A. 1994. *Corrosion of Epoxy-Coated Rebar on Florida Bridges*. Final Report. Tallahassee, FL: Florida Department of Transportation.

Scannell, W. T., A.A. Sohanghpurwala, and M. Islam. 1996. *FHWA-SHRP Showcase: Assessment of Physical Condition of Concrete Bridge Components*. Washington, D.C.: Federal Highway Administration.

Schlorholtz, S. 1998. *Report of X-ray Analysis*. Ames, IA: Iowa State University.

Smith, J. L. and Y. P. Virmani. 1996. *Performance of Epoxy Coated Rebars in Bridge Decks*. FHWA-RD-96-092. Washington, D.C.: Federal Highway Administration.

Weyers, R. E., W. Pyc, J. Zemajtis, Y. Liu, D. Mokarem, and M.M. Sprinkel. 1997. Field Investigation of Corrosion-Protection Performance of Bridge Decks Constructed with Epoxy-coated Reinforcing Steel in Virginia. *Transportation Research Record* 1597.

Weyers, R. E. 1995. *Protocol for In-Service Evaluation of Bridges with Epoxy-Coated Reinforcing Steel*. Final Report. Blacksburg, VA: National Cooperative Highway Research Program, Associated Materials Engineers.

Weyers, R.E., B.D Prowell, and M.M. Springkel. 1993. *Concrete Bridge Protection, Repair, and Rehabilitation Relative to Reinforcement Corrosion: A Methods Application Manual*. SHRP-S-360. Washington, D.C.: Strategic Highway Research Program, National Research Council.

Weyers, R.E., M.G. Fitch, E.P. Larsen, I.L. Al-Qadi, W.P. Chamberlin, and P.C. Hoffman. 1994. *Service Life Estimate*. Report SHRP-S-668. Washington, D.C.: Strategic Highway Research Program, National Research Council.

APPENDIX A. LIFE EXPECTANCY AND LIFE-CYCLE COST

The authors acknowledge that sufficient data have not yet been obtained to decisively predict the life expectancies and life-cycle costs for MMFX microcomposite and epoxy-coated mild steel reinforcement. However, as the monitoring of corrosion for MMFX and epoxy-coated reinforcement continues in the field bridge, a greater degree of certainty of the measured data will be established, and a more justified conclusion can be drawn about life expectancy and life-cycle costs. While the limited results from 40 weeks of laboratory testing do not constitute a prediction of life expectancy and life-cycle cost, a procedure is presented below for determining the life expectancy and life-cycle cost when definitive evidence is attained.

A.1. Life Expectancy

The life expectancy of bridge decks constructed with different steel reinforcing systems is estimated by the two-stage diffusion-spalling model (i.e., the time required for corrosion initiation plus the subsequent time required to cause spalling due to corrosion). In the following sections, a procedure is presented that can be used to estimate the life expectancy of a bridge deck.

A.1.1. Time to Corrosion Initiation

The time to corrosion initiation is estimated using Fick's Second Law of Diffusion and chloride ion concentrations at corrosion initiation, as measured in the current study.

Fick's Second Law of Diffusion is a common diffusion model used to determine the length of the initiation stage (i.e., the time required for the chloride ion to migrate through a bridge deck to the top steel reinforcement layer and accumulate to the chloride threshold value). The model assumes that the chloride ion diffuses through an isotropic medium (Weyers et al. 1994). The fundamental second order differential equation of Fick's Second Law of Diffusion is as follows:

$$\frac{\delta C}{\delta t} = D_c \frac{\delta^2 C}{\delta x^2} \qquad \text{(A.1)}$$

Where

C = chloride concentration with depth, in.
t = time, years
x = depth, in.
D_c = diffusion constant, sq. in./yr.

A closed-form solution of the above differential equation for a semi-infinite bridge deck (i.e., small ratio of depth to length or width of a bridge deck) can be expressed as follows (Brown 1980):

$$C_{(x,t)} = C_0\left\{1 - erf\left[\frac{x}{2\sqrt{(D_c t)}}\right]\right\} \quad \text{(A.2)}$$

Where

$C_{(x,t)}$ = measured chloride concentration at desired depth, lb./cu. yd.
C_0 = constant surface concentration measured at 1/2 in. below the bridge deck surface, lb./cu. yd.
t = time, years
x = depth measure from the bridge deck surface, in.

$$erf(y) = \frac{2}{\sqrt{\pi}}\int_0^y e^{-(s)^2}\,ds \quad \text{(A.3)}$$

The error function, *erf(y)*, is the integral of the Gaussian distribution function from 0 to y.

A.1.1.1. Surface Chloride Ion Constant

The application of Fick's Second Law of Diffusion to assess the time to corrosion initiation requires the determination of the surface chloride content, C_0, and the diffusion constant, D_c. Investigations of the chloride ion concentration in bridge decks have concluded that the concentrations measured 12.7 mm (1/2 in.) from the bridge deck surface reached a stable condition after four to six years of service (Weyers et al. 1994). For this reason, the surface chloride constant, C_0, in Equation (A.2) has been recommended to equal the measured chloride ion concentration at 12.7 mm (1/2 in.) from the bridge deck surface.

A.1.1.2. Chloride Diffusion Constant

The transport of chloride ion in bridge decks is assumed to be a one-dimensional diffusion process. However, the ingress of chloride ion in concrete is impacted by concrete capillaries and cracking. The quality of concrete affects the phenomenon of the diffusion process in terms of the time needed for chloride content to reach a certain depth and concentration. A strong correlation between the diffusion constant and the water-cement ratio has been observed in controlled experimental studies (Herald 1989). Earlier research also found temperature to have a significant impact on the diffusion process of chloride in hardened cement paste (Brown 1980). The omnipresent cracking that increases the rate of chloride diffusion is affected by many factors, such as water-cement ratio, temperature fluctuation, traffic volume, and the curing and construction process. Therefore, the chloride diffusion constant, D_c, in Equation (A.2) is commonly characterized by the construction practices dictated from state to state.

A.1.1.3. Reinforcement Cover Depth

Since rehabilitation will only take place after spalling or other deterioration has occurred, to calculate a realistic time for chloride ion to reach the reinforcement depth, the full functional

service life is used. By this reasoning, it is recommended that one not use the mean values of the cover depth, but instead a statistical value for cover depth that accounts for the possibility that some reinforcement could be located at a depth less than the mean value (Weyers 1995). This can be calculated as

$$x = \bar{x} + \alpha\sigma \qquad \text{(A.4)}$$

Where

$\bar{x}$ = mean steel reinforcement cover depth, in.
α = values corresponding to a given cumulative percentage
σ = standard deviation of the cover depth

The α value can be selected as the percent damage of the worst traffic lane. Statistical analysis of the measured cover depth taken from several bridge decks followed a normal distribution. Therefore, a standard normal cumulative probability table can be used to establish the α value.

Previous research was conducted to analyze of the diffusion constant and the surface chloride ion constant throughout the state of Iowa (Fanous, Wu, and Pape 2000). This database consists of concrete power samples collected from 81 bridge decks reinforced with epoxy-coated steel. An average concrete cover depth $\bar{x}$ = 69.60 mm (2.74 in.), associated with standard deviation σ = 11.28 mm (0.444 in.), was reported for bridge decks in the state of Iowa.

Research recommends using the α value corresponding to 11.5% visual damage (corrosion or delamination) to the reinforcement of the worst traffic lane of a bridge deck, as an indication of the end of the functional service life for a bridge deck (Weyers 1995). Based on this assumption that 11.5% of the reinforcement is contaminated by chloride ions, from a standard normal cumulative probability table the α value for calculating the top reinforcement layer depth is α = -1.2. Subsequently, the cover depth calculated from equation (A.4) is

$$x = 69.60 + (-1.2)(11.28) = 56.13\,\text{mm} \text{ or } x = 2.74 + (-1.2)(0.444) = 2.21\,\text{in.} \qquad \text{(A.5)}$$

Fanous, Wu, and Pape (2000) reported that bridge decks in the state of Iowa were found to have a diffusion constant D_c = 1.27 mm^2/yr (0.05 in^2/yr) and a mean surface chloride constant C_0 = 8.31 kg/m^3 (14.0 lb./cu. yd.) (Fanous, Wu, and Pape 2000). Substituting the cover depth x = 56.13 mm (2.21 in.), the diffusion constant D_c = 1.27 mm^2/yr (0.05 sq. in./yr), and the mean surface chloride constant C_0 = 8.31 kg/m^3 (14.0 lb./cu. yd.), equation (A.2) can be expressed as

$$C_{(x,t)} = 14.0\left\{1 - erf\left[\frac{2.21}{2\sqrt{(0.05t)}}\right]\right\} \qquad \text{(A.6)}$$

Where

$C_{(x,t)}$ = measured chloride ion concentration for the initiation of corrosion at depth of the top layer of reinforcement, lb./cu. yd.

t = time to be calculated for the initiation of corrosion, years

Equation (A.6) relates the time required for chloride ion to migrate to a depth of 2.21 in. and accumulate the required concentration to initiate corrosion for a respective reinforcement type. Substituting the chloride ion concentration at initiation in Equation (A.6), the time *t* can be calculated. This is the time to corrosion initiation for the top layer of steel reinforcement of a bridge deck.

A.1.2. Time between Corrosion Initiation and Spalling

Published literature indicates that estimating the length of time between corrosion initiation and spalling is a difficult task. However, a research study suggested using the rate at which a given reinforcement type corrodes as a means to estimate the length of this period (Pfeifer 2000). Equation (A.7) shows this linear relationship.

$$e = r \cdot t \tag{A.7}$$

Where

e = loss in reinforcing bar diameter, μm
r = corrosion rate, μm loss per unit time
t = time to be calculated between corrosion initiation and spalling, years

The research presenting this technique also stated that a critical value for the loss in reinforcing bar diameter of 0.025 mm (0.00098 in.) would result in a volume of corrosion products sufficient to crack concrete (Pfeifer 2000). Using this assumption, Equation (A.7) can be expressed as

$$25\mu m = r \cdot t \tag{A.8}$$

To determine the rate of corrosion for use in Equation (A.8), the corrosion current can be determined by measuring the voltage drop across the resistor (i.e., macrocell corrosion measurement). The corrosion current is calculated from Ohm's Law, Equation (A.9), which is equal to the voltage divided by the resistance.

$$I = \frac{V}{R} \tag{A.9}$$

Where

I = corrosion current, amperes
V = macrocell voltage, volts
R = resistance, ohms

The actual resistance of each 10-ohm resistor is measured separately. Once the current is calculated, the corrosion rate, in terms of metal loss, is calculated using Faraday's Law (Darwin et al. 2002).

$$r = \frac{ia}{nFD} \tag{A.10}$$

Where

r = corrosion rate, thickness loss per unit time
i = current density, amperes per cm^2
a = atomic weight, 55.84 g (1.97 oz) for mole iron
n = number of equivalents exchanged, 2 electrons transferred for Fe^{2+}
F = Faraday's constant, 96,485 coulombs per mole
D = density of metal, 7.87 g/cm^3 (4.55 oz/in^3) for steel

In terms of current density, i, in μA per cm^2, corrosion rate, r, in μm per year is

$$r = 11.59i \tag{A.11}$$

The calculated average 280-day (40-week) corrosion rates are shown in Table A.1 for MMFX, epoxy-coated reinforcement, and uncoated steel reinforcement, respectively.

From the macrocell corrosion measurement, an average corrosion rate can be determined by using equation (A.11). Substituting this corrosion rate, r, in Equation (A.8), the period of time, t, between corrosion initiation and spalling can be calculated. This is the time required for corrosion products on the reinforcement to accumulate to a volume sufficient to crack the concrete in a bridge deck. Through the combination of the time to corrosion initiation from Equation (A.6) and time from initiation to spalling from Equation (A.8), the time to the first repair for the respective reinforcement type is calculated.

Table A.1. Average corrosion rate from corrosion initiation

Specimen identification	Corrosion rate, μm/yr
A-L mmFX (1)	3.19
A-L mmFX (2)	
A-L mmFX (3)	
A-T mmFX (1)	
A-T mmFX (2)	
MMFX Average	*3.19*
A-L-UC (1)	17.18
A-L-UC (2)	12.92
A-L-UC (3)	8.12
A-T-UC (1)	9.04
A-T-UC (2)	13.13
UC Average	*12.08*
A-L-EC-AD (1)	
A-L-EC-AD (2)	
A-L-EC-AD (3)	
A-T-EC-AD (1)	0.00
A-T-EC-AD (2)	
EC-AD Average	*0.00*
A-L-EC-DH (1)	0.00
A-L-EC-DH (2)	0.00
A-L-EC-DH (3)	0.00
A-T-EC-DH (1)	0.00
A-T-EC-DH (2)	0.00
EC-DH Average	*0.00*
A-L-EC-CH (1)	0.00
A-L-EC-CH (2)	
A-EC-CH Average	*0.00*

A.2. Illustrative Example to Calculate the Life Expectancy of a Bridge Deck with Uncoated Mild Steel Reinforcement

The following example uses the two-stage diffusion-spalling model to illustrate how the above procedure can be used to estimate the life expectancy of a bridge deck reinforced with uncoated steel in the state of Iowa. The uncoated reinforcement values for chloride ion concentration at initiation, 0.63 kg/m^3 (1.06 lb./cu. yd.) and corrosion rate (12.08 μm/yr) are listed in Tables 6.1 and A.1, respectively.

A.2.1. Time to Corrosion Initiation

An average chloride ion concentration of 0.63 kg/m^3 (1.06 lb./cu. yd.) was obtained at the initiation of corrosion for all five specimens containing uncoated reinforcement. By substituting the chloride ion concentration at corrosion initiation 0.63 kg/m^3 (1.06 lb./cu. yd.) for $C_{(x,t)}$,

Equation (A.6) can be expressed as

$$1.06 = 14.0\left\{1 - erf\left[\frac{2.21}{2\sqrt{(0.05t)}}\right]\right\} \quad \text{(A.12)}$$

Solving for *t* yields a time of 15 years for the chloride ion to migrate to the top reinforcement depth and accumulate a concentration sufficient to initiate corrosion for uncoated reinforcement.

A.2.2. Time between Corrosion Initiation and Spalling

From the macrocell corrosion measurement, an average corrosion rate of 12.08 μm/yr over 252 days (36 weeks) was calculated for all five specimens containing uncoated reinforcement. By substituting the corrosion rate (12.08 μm/yr) for *r*, Equation (A.8) can be expressed as

$$25\mu m = 12.08\frac{\mu m}{yr} \cdot t \quad \text{(A.13)}$$

Solving for *t* yields a time of 2 years for corrosion products on the reinforcement to accumulate to a volume sufficient to crack concrete containing uncoated reinforcement. This value matches those obtained in earlier studies (Fanous, Wu, and Pape 2000). The combination of the calculated time to corrosion initiation and time from initiation to spalling results in 17 years to the first repair for uncoated reinforcement. This value matches those obtained in earlier studies (Darwin et al. 2002; Fanous, Wu, and Pape 2000).